Placenta Accreta Spectrum Disorders: Update and Pictorial Review of the SAR-ESUR Joint Consensus Statement for MRI

Krupa K. Patel-Lippmann, MD • Virginia B. Planz, MD • Catherine H. Phillips, MD • Joanna M. Ohlendorf, MD
Lisa C. Zuckerwise, MD • Mariam Moshiri, MD

Author affiliations, funding, and conflicts of interest are listed at the end of this article.
See the invited commentary by Jha and Lyell in this issue.

Placenta accreta spectrum (PAS) disorders are a major cause of maternal morbidity and mortality and are increasing in incidence owing to a rising rate of cesarean delivery. US is the primary imaging tool for evaluation of PAS disorders, which are most often diagnosed during routine early second-trimester US to assess fetal anatomy. MRI serves as a complementary modality, providing value when the diagnosis is equivocal at US and evaluating the extent and topography of myoinvasion for surgical planning in severe cases. While the definitive diagnosis is established by a combined clinical and histopathologic classification at delivery, accurate antenatal diagnosis and multidisciplinary management are critical to guide treatment and ensure optimal outcomes for these patients. Many MRI features of PAS disorders have been described in the literature. To standardize assessment at MRI, the Society of Abdominal Radiology (SAR) and European Society of Urogenital Radiology (ESUR) released a joint consensus statement to provide guidance for image acquisition, image interpretation, and reporting of PAS disorders. The authors review the role of imaging in diagnosis of PAS disorders, describe the SAR-ESUR consensus statement with a pictorial review of the seven major MRI features recommended for use in diagnosis of PAS disorders, and discuss management of these patients. Familiarity with the spectrum of MRI findings of PAS disorders will provide the radiologist with the tools needed to more accurately diagnose this disease and make a greater impact on the care of these patients.

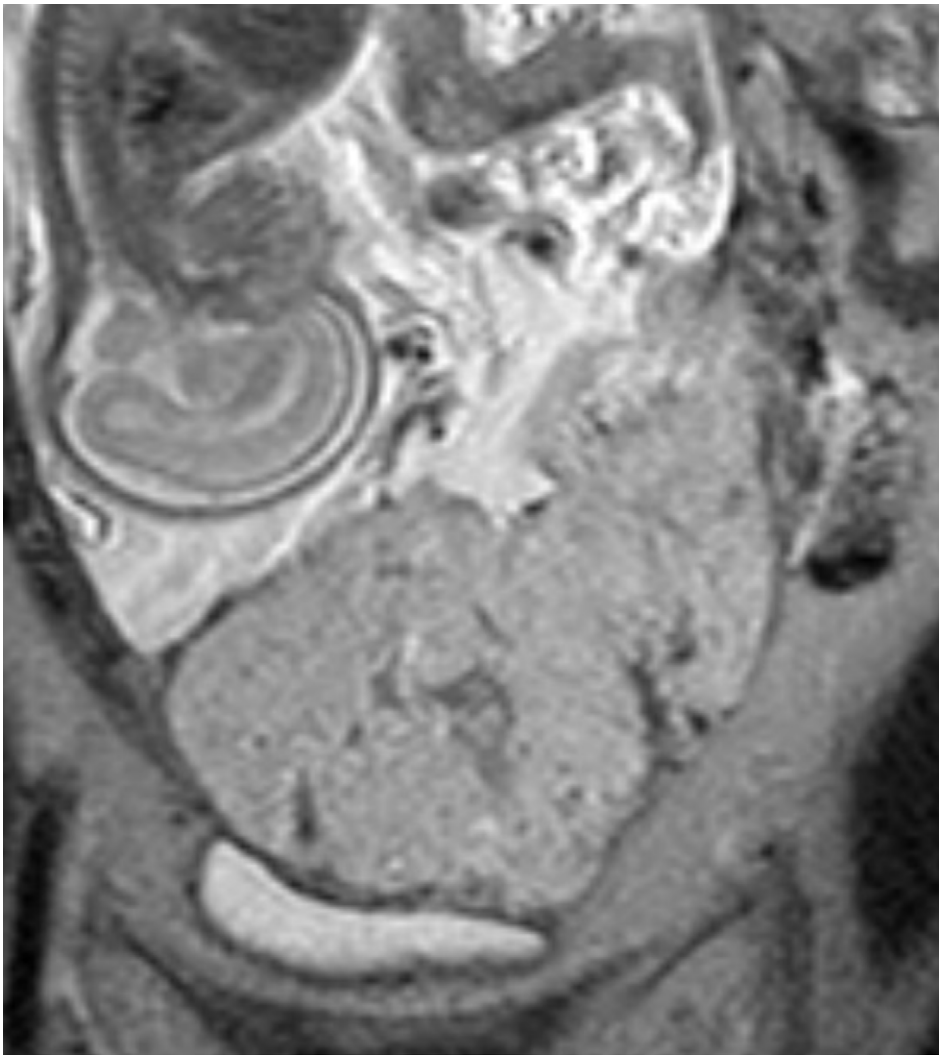

Invited Commentary
Supplemental Material
Quiz questions for this article are available through the Online Learning Center.
CME

RadioGraphics 2023; 43(5):e220090
https://doi.org/10.1148/rg.220090

Content Codes: MR, OB, US

Abbreviations: DWI = diffusion-weighted imaging, ESUR = European Society of Urogenital Radiology, FIGO = International Federation of Gynecology and Obstetrics, PAS = placenta accreta spectrum, SAR = Society of Abdominal Radiology, SPP = Society for Pediatric Pathology, SSFP = steady-state free precession

TEACHING POINTS

- The optimal time for evaluation of PAS disorders is 28–32 weeks gestation. Evaluation before 28 weeks gestation is limited owing to incomplete placental maturity and can be challenging after 32 weeks gestation owing to overlapping features of normal late gestation and PAS disorders.
- While no single feature allows diagnosis of PAS disorders, the combination of features and the presence of multiple features in the context of clinical risk factors increases the likelihood of underlying PAS disorder.
- Both intraplacental bands and blood vessels are hypointense on T2-weighted images; however, they can easily be distinguished on balanced SSFP images. Vessels will be T2 hyperintense, and bands will remain T2 hypointense.
- Myometrial thinning is defined as thinning of the myometrium over the placenta to less than 1 mm or not visible at all. Loss of the normal trilaminar appearance can be present in a normal placenta, especially late in gestation; however, the T2-hypointense line should remain intact.
- Involvement of critical structures—such as the bladder, bowel, parametrium, pelvic sidewall, ureters, and abdominal wall—and the relationship to major vessels, especially the internal iliac vasculature, are critical to the surgical approach and multidisciplinary surgical team engagement for delivery.

Introduction

Placenta accreta spectrum (PAS) disorders are the result of pathologic implantation of the placenta into the myometrium. PAS disorders are hypothesized to be caused by a defect of the endometrial-myometrial interface, leading to failure of normal decidualization (1). This results in trophoblastic migration and abnormal attachment or invasion of the placental chorionic villi directly to the underlying myometrium, with subsequent failure of placental separation from the uterus at the time of delivery (1).

The incidence of PAS disorders has increased almost 10-fold in the past 50 years. The reported incidence of PAS disorders from 2015 to 2017 in patients undergoing cesarean section in the United States was 0.29%, with up to one in 313 of all deliveries affected by the end of 2017 (2). PAS disorders are a major cause of maternal morbidity and mortality, typically owing to massive obstetric hemorrhage, with 52% requiring peripartum hysterectomy (3–5).

Major risk factors for PAS disorders include placenta previa, prior cesarean section, and history of prior PAS disorder. Additional risk factors include multiparity, prior uterine surgery (including dilation and curettage [D&C] and myomectomy), endometrial ablation, pelvic irradiation, uterine artery embolization, advanced maternal age, infertility, and use of assisted reproductive technologies (6). The common feature in many of these risk factors is uterine scarring or injury, which predisposes to PAS disorders.

Repeat cesarean section is associated with a progressively increased risk of PAS disorders. The risk increases from 0.2% after one cesarean section to 0.3%, 0.6%, 2.1%, 2.3%, and 6.7% after two to six cesarean sections, respectively, if placenta previa is absent (7). In the presence of placenta previa, the risk increases substantially to 3%, 11%, 40%, 61%, and 67% for one to five cesarean sections, respectively (7). The marked increase in the incidence of PAS disorders over the past several decades has been largely attributed to an increasing number of deliveries via cesarean section, which now accounts for nearly one-third of all deliveries, compared with 12% in 1982 (8–10).

PAS disorders has been endorsed as the most inclusive term to describe this spectrum of disease, with terms such as *morbidly adherent placenta* or *invasive placentation* falling out of favor (11,12).

PAS disorders range in severity from superficial adhesion of placental villi to the myometrium (placenta accreta) to varying degrees of myometrial invasion (placenta increta or placenta percreta) (6). Placenta percreta has traditionally been described as transmural invasion through the serosa with potential extension into adjacent organs such as the bowel, bladder, or abdominal wall. A recent systematic review found that nearly 62% of cases of PAS disorders were myoadherent (placenta accreta), whereas myoinvasive disease (placenta increta and placenta percreta) represented 16% and 22% of cases of PAS disorders, respectively. However, accurate estimation of prevalence was limited by the large amount of heterogeneity in both clinical and histopathologic diagnosis of this disease in the literature (3).

The more recent literature has challenged the concept of transmural villous tissue invasion and questioned the existence of placenta percreta, recognizing that surgical manipulation and dissection can lead to a pathologic appearance of villous tissue crossing the serosa. As such, the traditionally used terminology of *placenta accreta*, *placenta increta*, and *placenta percreta* is becoming less accepted, with the focus rather on identification of myoadherent versus myoinvasive disease (13,14).

Definitive diagnosis of PAS disorders occurs at delivery by using combined clinical and histopathologic diagnostic criteria per the recently updated International Federation of Gynecology and Obstetrics (FIGO) classification system (Fig 1) (6,11,12,15–17). The FIGO classification is largely based on surgical findings during laparotomy, categorized as grades 1–3, representing adherent placenta (grade 1) and invasive placenta (grades 2 and 3), with corresponding histologic criteria. Myoinvasive placenta is considered grade 2 if the serosa is intact and grade 3 if there is involvement of the serosa. Grade 3 is further subdivided into serosal involvement (grade 3a), bladder invasion (grade 3b), and invasion of other pelvic tissues or organs (grade 3c).

In parallel, the Society for Pediatric Pathology (SPP) has developed standardized terminology for histopathologic diagnosis of PAS disorders, also classified into three descriptive subgroups, grades 1–3, representing noninvasive disease (grade 1), superficial invasion with 25% of wall thickness preserved (grade 2), and deep invasion (grade 3) (Fig 1).

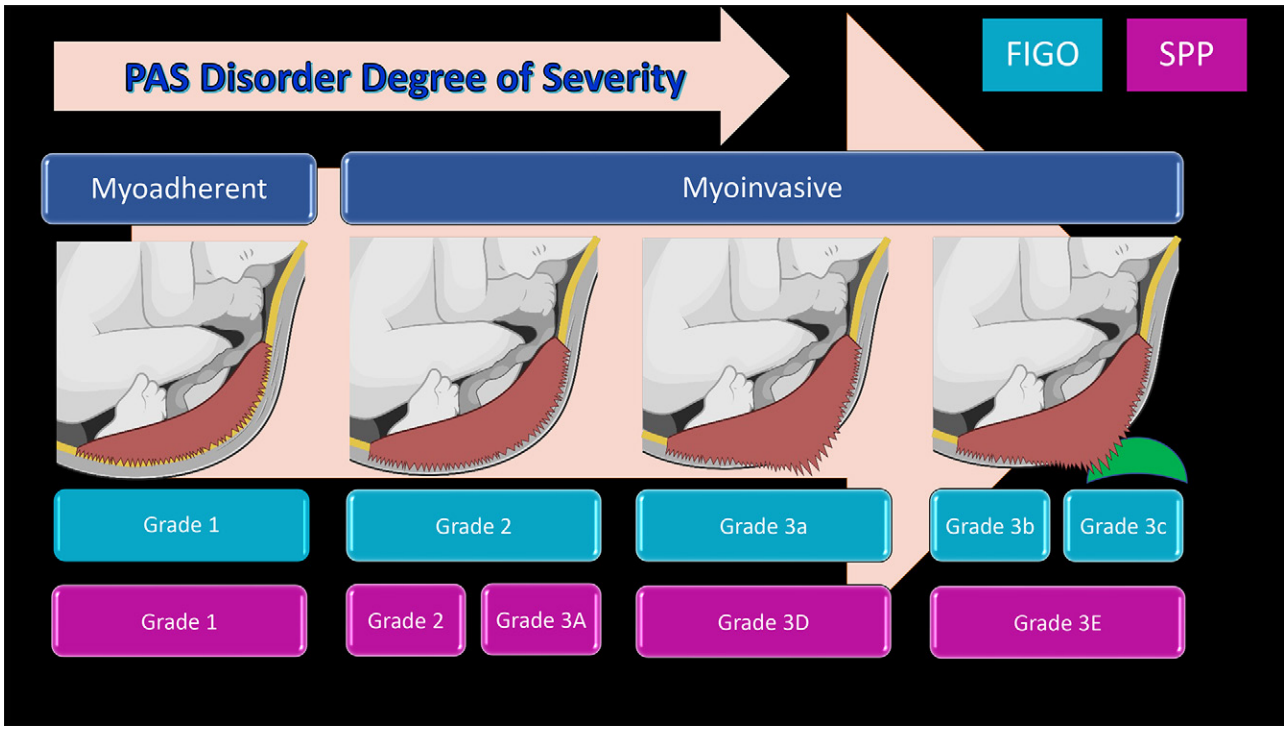

Figure 1. FIGO classification (light blue boxes) and Society for Pediatric Pathology (SPP) pathologic classification (purple boxes) of PAS disorders. Brown = placenta, yellow = endometrium, gray = myometrium. Grade 1 represents myoadherent disease in both classifications. Myoinvasive disease without serosal involvement is FIGO grade 2, subdivided by SPP into grades 2 and 3A depending on the degree of myoinvasion. Myoinvasive disease with serosal involvement is FIGO grade 3a and SPP grade 3D. Myoinvasive disease with extrauterine invasion (green) is SPP grade 3E, subdivided by FIGO into grades 3b (bladder) and 3c (other tissue or organs). Extrauterine invasion includes both fibroadipose tissue (as in broad ligament or pelvic sidewall involvement) and organ invasion (most commonly the bladder).

Deep invasion is subcategorized by intact serosa (grade 3A), disrupted serosa (grade 3D), and extrauterine invasion into organs or fibroadipose tissue (grade 3E) (18). While histopathologic diagnosis is considered the standard of reference for confirming the diagnosis, correlation with the surgical findings is required (15). Histologic evaluation results may not be available for some cases of adherent placenta or those managed conservatively, emphasizing the importance of the multidisciplinary correlation (15).

Accurate preoperative detection of PAS disorders with imaging, specifically the depth and location of myoinvasion and extrauterine involvement, is critical for presurgical planning and optimizing patient outcomes. US is the first-line imaging tool for detection, while MRI is increasingly being used in conjunction with US for both diagnosis and surgical planning. A large portion of the imaging literature has been dedicated to identifying MRI features that suggest PAS disorders; however, many of these described "signs" have variable terminology and descriptions (19–26).

In 2020, in an effort to provide unified terminology and standardization paralleling efforts by FIGO and SPP, the Society of Abdominal Radiology (SAR) and European Society of Urogenital Radiology (ESUR) released a joint consensus statement based on data and expert opinion for MRI evaluation of PAS disorders (27). This statement provides guidance for MR image acquisition and interpretation and a reporting lexicon and describes seven MRI features that met consensus and are recommended for diagnosis of PAS disorders.

In this article, we provide an overview of the role of US and MRI in diagnosis of PAS disorders, review the SAR-ESUR joint consensus statement on MRI recommendations and imaging features, and review management of these patients, including the potential role of MRI in the postpartum period.

Normal Anatomy of Placenta at US and MRI

The placenta is formed embryologically from the outer trophoblast cells of the blastocyst. These cells differentiate into the inner proliferative cytotrophoblast and the outer-layer syncytiotrophoblast, which erode into maternal tissues as well as secrete human chorionic gonadotropin (hCG) to maintain the pregnancy, as the progesterone production from the corpus luteum declines during the first trimester (28–30). The blastocyst implants within the endometrial canal, usually within the mid to upper half of the uterine cavity. Placental tissue is typically visible at 10 weeks gestation at transabdominal or transvaginal US. Intervillous blood flow is seen at Doppler US as early as 12–13 weeks gestation, and the placenta is well formed by 14–15 weeks gestation (31,32).

At US, the normal placenta appears as a homogeneously hyperechoic structure opposed to the myometrium, with a thin (1–2-mm) intervening hypoechoic or anechoic retroplacental clear zone containing the retroplacental complex (Fig S1, Movie 1). This complex consists of the decidua basalis, maternal vessels, and myometrium. The placenta continues to increase in size in the second trimester and may contain

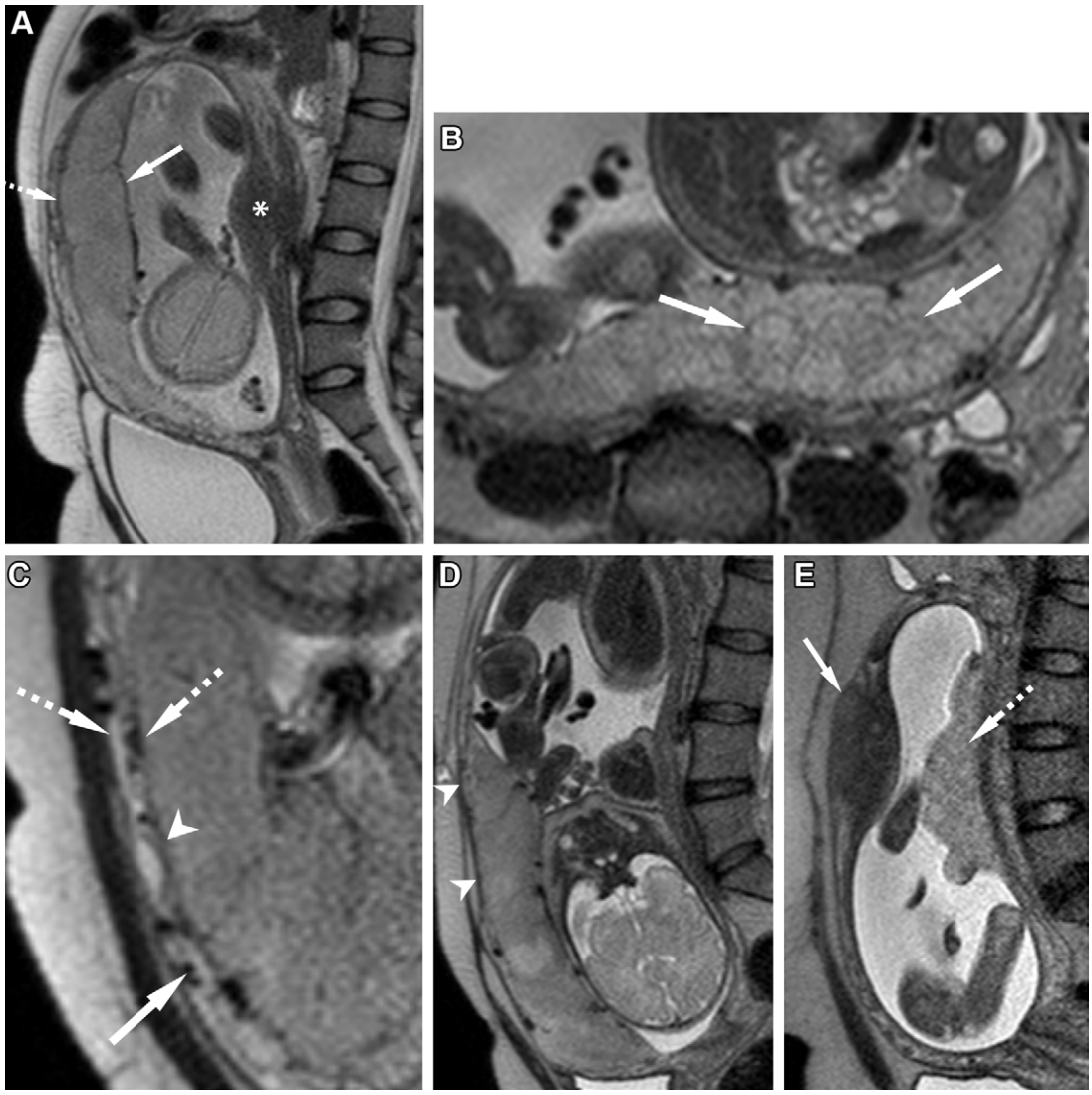

Figure 2. MRI of normal placenta. **(A)** Sagittal T2-weighted image through the uterus at 26 weeks gestation shows an anterior placenta with smooth uniform contours (solid arrow). Note the homogeneous moderate T2 signal hyperintensity relative to the myometrium (*) as well as the normal interface between the placenta and myometrium (dashed arrow). **(B)** Axial T2-weighted image in another patient at 30 weeks gestation shows thin T2-hypointense septa (arrows) coursing through the normal placenta. **(C)** Cropped sagittal T2-weighted image in another patient at 30 weeks gestation shows the uteroplacental interface. Note the trilaminar myometrium (dashed arrows), with a T2-hypointense inner layer, T2-intermediate-signal-intensity middle layer, and T2-hypointense outer layer. The placental contour is smooth and uniform, with a well-defined and preserved T2-hypointense inner layer (arrowhead) with normal retroplacental vascularity and flow voids (solid arrow). **(D)** Normal third-trimester placenta in a 33-year-old patient at 35 weeks gestation. Sagittal T2-weighted image shows normal myometrial thinning (arrowheads) and loss of the trilaminar appearance in late gestation. The single T2-hypointense line reflects a combination of the preserved inner and outer layers with compression of the intervening vascular layer. **(E)** Sagittal T2-weighted image in another patient shows a normal posterior placenta (dashed arrow) with a focal myometrial contraction anteriorly (solid arrow).

venous lakes with smooth contours and slow internal flow at Doppler imaging. The placenta becomes increasingly vascular in the third trimester and can develop calcifications, reflecting expected placental aging. At term, it measures 12–20 cm in diameter and 2–4 cm in thickness (32).

At MRI, the placenta is discoid in morphology with smooth tapered margins and homogeneous moderately hyperintense signal intensity on T2-weighted images relative to the myometrium (Fig 2A). Blaicher et al (33) reviewed 100 normal placentas at MRI and found that over 85% retained homogeneous signal intensity from 19 to 23 weeks gestation, with 90.7% demonstrating mild lobulation and heterogeneity, which increased with gestational age. This increasing heterogeneity may be related to expected normal morphologic changes related to placental aging and may reflect areas of infarction and calcification, findings that are seen in a portion of normal placentas at term (33). Thin T2-hypointense septa surrounding placental cotyledons can often be seen coursing through the normal placenta (Fig 2B).

The adjacent myometrium at the uteroplacental interface is best seen on T2-weighted images and steady-state free precession (SSFP) images and demonstrates a trilaminar appearance, with a T2-hypointense inner layer, T2-intermediate-signal-intensity middle layer, and T2-hypointense outer serosal layer (34) (Fig 2C). This trilaminar appearance is often lost in late gestation, with a preserved single T2-hypointense line reflecting a combination of the inner and outer layers and compression of the intervening vascular layer (Fig 2D). Morphologically, the uterus demonstrates an inverted pear-shaped appearance without bulging inferiorly.

Myometrial contractions are often seen in gravid patients, which appear as focal low-T2-signal-intensity thickening of the myometrium and distortion of the inner myometrial contour (Fig 2E). Contractions may be seen anywhere in the uterus, including at the uteroplacental interface, and should not be misinterpreted as pathologic, with consecutively performed sequences often showing resolution of this finding.

Role of US in Diagnosis of PAS Disorders

Every patient receiving routine prenatal care will undergo an early second-trimester US examination to assess fetal anatomy, which is also an opportune time to evaluate for placental findings, including location and imaging features of PAS disorders. Patients with risk factors for PAS should receive

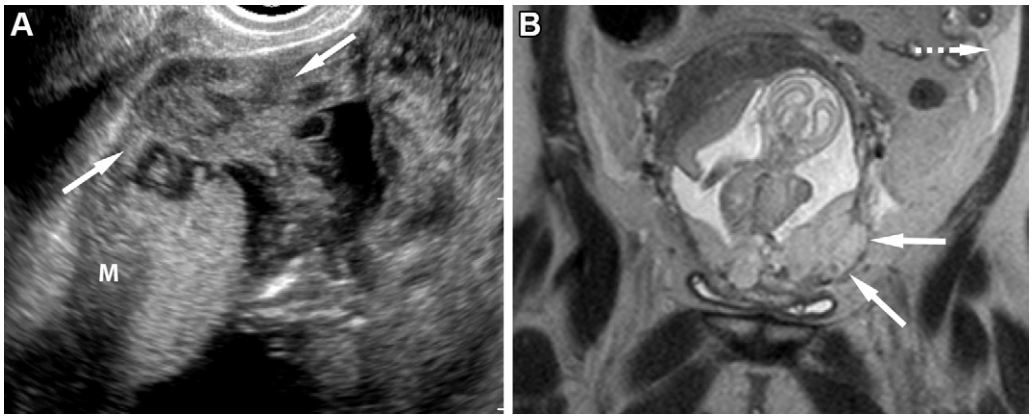

Figure 3. Myoinvasive PAS disorder in the setting of an undiagnosed cesarean section scar pregnancy in a 36-year-old patient with a history of three prior cesarean sections. **(A)** Long-axis gray-scale transvaginal US image at 14 weeks gestation shows bulging of the lower uterine segment myometrial contour *(M)* with placenta extending through the serosa at the scar (arrows). Subsequent MRI was performed after transfer of care at 18 weeks gestation when the patient presented with vaginal bleeding. **(B)** Coronal T2-weighted image shows an exophytic mass (solid arrows) beyond the uterine serosa toward the left pelvic sidewall with small-volume hemoperitoneum (dashed arrow). An emergent hysterectomy with the fetus in situ was performed with intraoperative findings of active bleeding from the placenta, which was extending through the serosa on the left anterior margin.

a detailed assessment for PAS disorders at this time. US is a sensitive and specific screening test for PAS disorders, with a recent meta-analysis showing sensitivity of 83.3%–90.7% and specificity of 83.4%–97.0% (35,36). In their meta-analysis, Pagani et al (37) showed sensitivity for identification of placenta accreta, placenta increta, and placenta percreta of 91%, 93%, and 81% and specificity of 97%, 98%, and 99%, respectively, demonstrating the utility of US across the spectrum of PAS disorders (37).

Features of PAS disorders can also be seen in the first trimester. Low anterior implantation near or at the site of a prior hysterotomy is concerning for cesarean scar pregnancy, a precursor to severe PAS disorders (38,39). A portion of the PAS disorders that are seen in the second trimester is likely missed cesarean section scar pregnancies (Fig 3).

Recent studies suggest that screening for and diagnosis of PAS disorders can be achieved at 11–16 weeks with accuracy as high as 93%, using a two-stage strategy for early prediction (39,40). In this model, patients at high risk—defined as low-lying placenta and history of uterine intervention—after the 11–13-week nuchal translucency scan were sent for a second-stage assessment at a PAS clinic at 12–16 weeks, including a focused US examination to identify US markers of PAS disorders. When identified, findings of PAS disorders should be clearly documented in the US report and communicated to the clinical team. While reporting practices vary by institution, standardized US criteria and descriptors for PAS disorders are available and can be used to develop specialized templates and harmonize institutional reporting (41,42).

Sonographic findings of PAS disorders include the presence of abnormal placental lacunae, loss of the retroplacental clear zone, myometrial thinning, placental bulge, bladder wall interruption, focal exophytic mass, and abnormal vascularity at color Doppler US (41–43) (Table 1). Of note, all findings are not required for diagnosis of PAS disorders. The presence of placental lacunae and bladder wall disruption are the most specific sonographic findings of PAS disorders (44). Color Doppler US is a helpful adjunct in assessment for PAS disorders, with bridging vessels perpendicular through the placenta and toward the bladder considered highly indicative of PAS disorders (45,46). Sonographic evaluation for PAS disorders may be limited in the setting of elevated body mass index and posterior placental location, both of which require higher levels of technical expertise.

Role of MRI in Diagnosis of PAS Disorders

MRI can provide further evaluation of equivocal US findings and aid in surgical planning, especially in cases of suspected deep myoinvasion, as MRI accurately depicts the depth and topography of invasion (36,47,48). MRI is also valuable in assessment of posterior placenta. A recent meta-analysis showed recognition of 52% of posterior PAS disorder cases with prenatal US alone versus 73.5% if prenatal MRI was used (49). US and MRI otherwise have similar diagnostic accuracy for PAS disorders (35,36). Several recent meta-analyses show overall MRI sensitivity of 86.5%–94.4% and specificity of 96%–98.8% in prediction of the depth of placental invasion (35,36,48). These data should be interpreted with caution owing to the introduced bias of high pretest possibility, as only those with suspected PAS disorders undergo MRI (17).

The accuracy of MRI can be affected by the timing of imaging, as the myometrium naturally becomes thinner with progression of pregnancy and can mimic pathologic thinning (50). The optimal time for evaluation of PAS disorders is 28–32 weeks gestation. Evaluation before 28 weeks gestation is limited owing to incomplete placental maturity and can be challenging after 32 weeks gestation owing to overlapping features of normal late gestation and PAS disorders (50). Patients may present to higher levels of care after this time frame, and MRI should still be performed if indicated and the results interpreted in this context. Similarly, patients with

Table 1: US Findings of PAS Disorders

US Finding	Description
Gray-scale US features	
Abnormal placental lacunae	Presence of multiple lacunae, which are large irregularly shaped placental hypoechoic spaces that give the placenta a moth-eaten appearance; they can contain internal turbulent flow at gray-scale US Lacunae are usually centered within a lobule or cotyledon and are adjacent to the involved myometrium These are not to be confused with placental lakes, which are features of a normal placenta and appear as a few small hypoechoic spaces with regular margins scattered throughout the placental tissue with slow flow (Movie 2)
Loss of retroplacental clear zone	Marked by obliteration or irregularity of the hypoechoic plane between the placenta and myometrium This area can be falsely obscured by pressure from a distended urinary bladder and excess pressure from the ultrasound transducer
Myometrial thinning	Asymmetric thinning of myometrium overlying the placenta relative to myometrium not covered by placenta This can be focal or diffuse, with the myometrium measuring <1 mm or being nonvisible It is associated with prior hysterotomy scars or placental invasion
Placental bulge (Fig S2)	Focal bulge of the placenta in an area of myometrial thinning, leading to deviation of the uterine serosa from its expected plane and uterine contour deformity
Bladder wall interruption (Fig S3)	Disruption of the normally smoothly echogenic bladder wall, located between the uterine serosa and urinary bladder lumen
Focal exophytic mass	Focal extension of placental trophoblastic tissue beyond the uterine serosa, most commonly into the bladder
Color Doppler US features	
Bridging vessels	Perpendicularly oriented vessels seen extending from the placenta through the underlying myometrium and into the uterine serosa or extrauterine structures, including but not limited to the bladder
Uterovesical hypervascularity	Increased color Doppler signal between the myometrium and posterior bladder wall, which likely indicates increased vascular density and tortuosity in that region
Subplacental hypervascularity (Fig S4)	Increased color Doppler signal in the placental bed, which likely indicates increased vascular density and tortuosity in that region
Placental lacunae feeder vessels (Fig S5)	Vessels with high-velocity blood flow extending from the myometrium into lacunae, creating turbulent flow within the lacunae

concerning findings at early anatomic imaging do not need to wait until 28 weeks gestation, as these patients can present with life-threatening bleeding at any time in pregnancy, with clinical indications driving appropriate timing of imaging.

Reader experience also plays a role in the diagnostic accuracy of MRI, with experienced readers often performing better (51–53). While MRI capabilities and expertise may not be available in all resource settings, a 2017–2018 international survey of practices of FIGO expert panel members showed increasing use of MRI for diagnosis of PAS disorders, with over 61% using both US and MRI (11,54).

MRI Protocol

Sample protocols for 1.5-T and 3-T MRI are provided, adapted from the SAR-ESUR consensus statement (Table 2) (27). Multiplanar non–fat-saturated T2-weighted imaging through the placenta is the primary sequence used in evaluation of PAS disorders. All suspected abnormalities should be confirmed in two planes to avoid misinterpretation of partial volume averaging resulting from the physiologic curvature of the uterus. Fat-saturated T1-weighted imaging is useful to evaluate for uterine and placental hemorrhage. Optional sequences include SSFP, which is useful for vascular assessment of the placenta, and diffusion-weighted imaging (DWI), which may help define the placental-myometrial interface in the setting of myometrial engorgement (Fig 4) (55).

The supine position is preferred for the examination and is usually well tolerated in the second trimester. The left lateral decubitus position can be considered during the third trimester or if there is significant discomfort or concern for inferior vena cava (IVC) compression. Moderate distention of the bladder is ideal for assessment of bladder involvement. Breath-holding techniques should be performed to diminish motion artifact. Use of a multichannel phased-array surface coil is recommended. Administration of gadolinium-based intravenous contrast material is not recommended for evaluation of PAS disorders during gestation (56).

Per American College of Radiology (ACR) guidelines, placental MRI can be safely performed at 1.5 T and 3 T at normal operating mode specific absorption rate levels (<2 W/kg) for a duration of less than 30 minutes (57). Currently, there is no documented evidence of harmful effects to the fetus when exposed to 1.5-T or 3-T MRI. Potential harms raised in the past literature include acoustic damage and teratogenic effects related to tissue heating, but there are no published data confirming these concerns. Recent retrospective series have shown no adverse effects on fetal growth or neonatal hearing (58,59).

MRI Features of PAS Disorders: SAR-ESUR Consensus Statement

The SAR-ESUR consensus statement recommends seven features for diagnosing PAS disorders, which are reviewed in this

Table 2: 1.5-T and 3-T MRI Protocols for Evaluation of PAS Disorders

Sequence by Field Strength	Plane	Field of View (mm)	Section Thickness (mm)	TR/TE (msec)	Flip Angle (degrees)	Matrix
1.5-T field strength						
T2W half-Fourier	Axial	320–400	4	800/85	120	320 × 216
T2W half-Fourier	Sagittal	430	4	800/87	120	384 × 256
T2W h alf-Fourier	Coronal	430	4	800/87	120	384 × 256
SSFP*	Axial	320–400	4	3.31/1.36	60	256 × 192
SSFP*	Sagittal	320–400	4	3.51/1.41	60	320 × 270
SSFP*	Coronal	320–400	4	3.51/1.41	60	320 × 270
T1W 3D fat-saturated	Axial	320–400	3	4.35/1.61	10	256 × 192
T1W 3D fat-saturated	Sagittal	320–400	3	4.27/1.56	10	256 × 256
DWI*	Axial or sagittal	320–400	5	3200/75	10	256 × 192
3-T field strength						
T2W half-Fourier	Axial	320–400	4	800/85	120	320 × 216
T2W half-Fourier	Sagittal	430	4	800/87	120	384 × 256
T2W half-Fourier	Coronal	430	4	800/87	120	384 × 256
SSFP*	Axial	320–400	4	4.66/1.93	60	256 × 192
SSFP*	Sagittal	320–400	4	4.66/1.93	60	320 × 270
SSFP*	Coronal	320–400	4	4.66/1.93	60	320 × 270
T1W 3D fat-saturated	Axial	320–400	3	4.2/1.2	10	256 × 192
T1W 3D fat-saturated	Sagittal	320–400	3	4.2/1.2	10	256 × 256
DWI*	Axial or sagittal	320–400	5	3200/75	90	256 × 192

Note.—Planes should be set up relative to the uterus, with oblique axial T2-weighted images obtained perpendicular to the placental-myometrial interface. DWI = diffusion-weighted imaging, TE = echo time, 3D = three-dimensional, T1W = T1-weighted, TR = repetition time, T2W = T2-weighted.
* Sequences considered optional per the consensus statement (27).

section. These include intraplacental T2-dark bands, placental or uterine bulge, myometrial thinning, bladder wall interruption, focal exophytic mass, loss of T2-hypointense retroplacental line, and abnormal vascularization of the placental bed. While no single feature allows diagnosis of PAS disorders, the combination of features and the presence of multiple features in the context of clinical risk factors increases the likelihood of underlying PAS disorder.

The goals of imaging are to identify findings supportive of PAS disorders, identify the presence or absence of myoinvasion, and outline the topography of myoinvasion, if present. Depth and topography are the main determinants of surgical outcome in patients with PAS disorders. Topography refers to the spatial delineation and anatomic location of myoinvasion, extrauterine spread, and adjacent organ invasion. Topography is a more reliable predictor of surgical morbidity than depth of invasion (60).

Imaging Features

Intraplacental Dark Bands.—Intraplacental bands are irregular T2-dark bands, ranging in size from 6 to 20 mm, which typically extend from the maternal surface and represent fibrin deposition from hemorrhage and infarct (20,21,24,27) (Figs 5C, 5D, 6, 7C, 7D, 8B, 9C, 9D, 10B, 11B, 12A). This is in contrast to the thin T2 septa seen in a normal placenta (Fig 2B). Intraplacental dark bands are the most sensitive MRI feature for PAS disorders, with high diagnostic sensitivity of 89.7%, 89.7%, and 82.6% and moderate specificity of 49.5%, 63.4%, and 58.5% for placenta accreta, placenta increta, and placenta percreta, respectively (48). An increasing volume of bands is associated with increased depth of placental involvement (19).

Both intraplacental bands and blood vessels are hypointense on T2-weighted images; however, they can easily be distinguished on balanced SSFP images. Vessels will be T2 hyperintense, and bands will remain T2 hypointense (23) (Fig 6). Similarly, areas of suspected T2-dark bands should be correlated with the findings on T1-weighted images to exclude hemorrhage mimicking bands. Finally, if the examination is performed late in gestation, small focal placental infarcts can be considered normal (33). Large areas of placental infarcts—particularly those not overlying the cervix—should raise suspicion and alert the radiologist to look for additional features of PAS disorders.

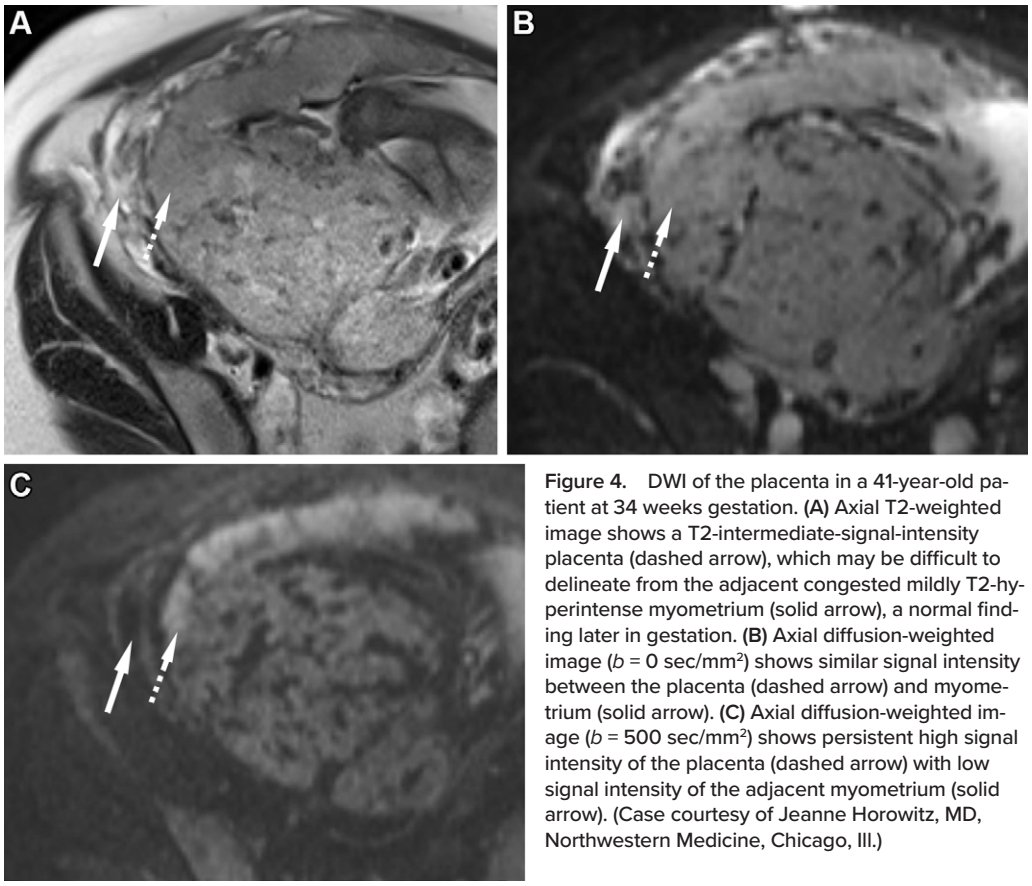

Figure 4. DWI of the placenta in a 41-year-old patient at 34 weeks gestation. **(A)** Axial T2-weighted image shows a T2-intermediate-signal-intensity placenta (dashed arrow), which may be difficult to delineate from the adjacent congested mildly T2-hyperintense myometrium (solid arrow), a normal finding later in gestation. **(B)** Axial diffusion-weighted image (b = 0 sec/mm^2) shows similar signal intensity between the placenta (dashed arrow) and myometrium (solid arrow). **(C)** Axial diffusion-weighted image (b = 500 sec/mm^2) shows persistent high signal intensity of the placenta (dashed arrow) with low signal intensity of the adjacent myometrium (solid arrow). (Case courtesy of Jeanne Horowitz, MD, Northwestern Medicine, Chicago, Ill.)

Uterine-Placental Bulge.—Uterine bulge involves deviation of the uterine serosa from the expected plane, which is caused by abnormal bulging of the placenta toward adjacent organs (20,24) (Figs 5C, 5D, 7C, 7D, 8C, 9C–9E, 10B, 10C, 11B). The uterine serosa remains intact; however, the uterine shape is morphologically distorted. Often, there is widening of the lower uterine segment due to myometrial remodeling, resulting in an hourglass configuration as opposed to the normal inverted pear-shaped uterus (Fig 9E) (23,27). Placental bulge has been shown to be an independent predictor of myoinvasive severe PAS disorder, with sensitivity of 76.7% and specificity of 62.5% for placenta increta and sensitivity of 77.4% and specificity of 64.7% for placenta percreta (48,61). Uterine placental bulge in conjunction with other findings of PAS disorder is 100% predictive of myometrial invasion; however, the uterine bulge sign alone without other features can lead to false-positive results, particularly given the reported fair to moderate interobserver variability for this feature (61,62).

Myometrial vascular congestion, a finding seen in both normal pregnancies and PAS disorders, can make delineation of the placental contour difficult and can mimic a bulge. The myometrium may appear mildly T2 hyperintense, blending in with the adjacent placenta and creating the appearance of a bulge (Figs 7C–7E). DWI can be helpful in this setting, as it may allow better delineation of the myometrial-placental interface compared with T2-weighted imaging, taking advantage of the intrinsic signal intensity differences between the high-signal-intensity placenta and low-signal-intensity myometrium on high-b-value images (Fig 4) (55).

Myometrial Thinning.—Myometrial thinning is defined as thinning of the myometrium over the placenta to less than 1 mm or not visible at all (26) (Figs 5C, 5D, 7C–7E, 8C, 9C–9E, 10B, 10C, 11B, 12A). Loss of the normal trilaminar appearance can be present in a normal placenta, especially late in gestation; however, the T2-hypointense line at the serosal margin should remain intact (Fig 2D) (23,27). Therefore, this sign should be used only in conjunction with other findings supportive of PAS disorders, particularly if imaging is performed after 32 weeks gestation (27). Focal myometrial interruption has good sensitivity and specificity for placenta accreta, placenta increta, and placenta percreta, ranging from 63.6% to 71.5% and from 70.2% to 74.6%, respectively (48).

There are several pitfalls to be aware of when evaluating for myometrial thinning. Nonpathologic myometrial thinning can often be seen in areas of myometrial compression, such as between the uterus and the maternal spine (23). Additionally, in patients who have undergone repeat cesarean sections, there can be widening of the old thin scar during pregnancy due to dehiscence of the lower uterine segment. In such cases, the placenta extends to the expected serosal margin at imaging, mimicking myometrial thinning and possibly being mistaken for a myoinvasive PAS disorder. Correlatively at delivery, the placenta may be visualized intraoperatively through this "uterine window" (63). However,

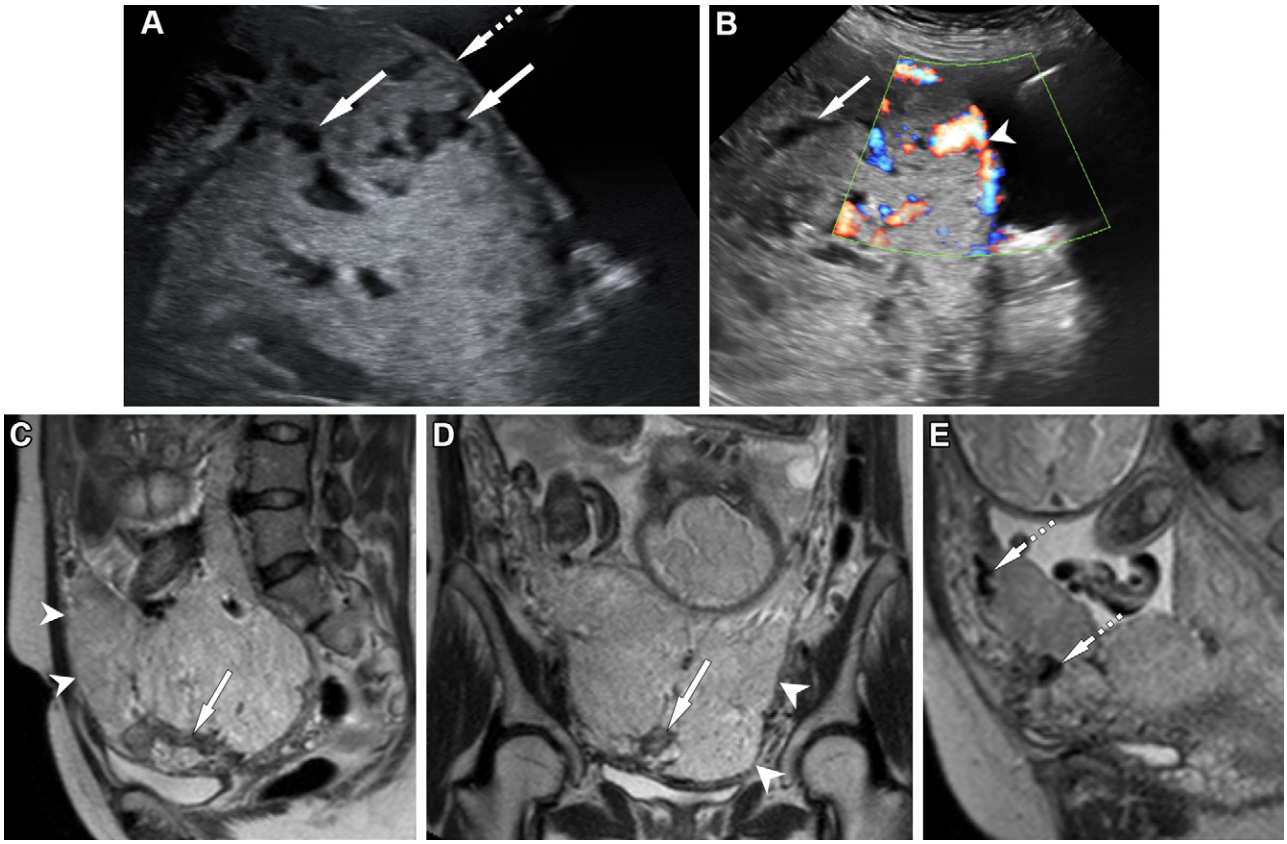

Figure 5. Myoinvasive PAS disorder in a 33-year-old patient with a history of two prior cesarean sections who was diagnosed with placenta previa. **(A, B)** Long-axis transabdominal gray-scale **(A)** and color Doppler **(B)** US images of the placenta at 34 weeks gestation show multiple clustered placental lacunae (solid arrows), with overlying myometrial thinning (dashed arrow in **A**) and increased vascularity at the uterovesical interface (arrowhead in **B**). **(C, D)** Sagittal **(C)** and coronal **(D)** T2-weighted images of the uterus show placenta previa associated with anterior myometrial thinning and uterine bulge (arrowheads). There is loss of the T2-hypointense retroplacental line with preservation of the thin T2-hypointense serosa. Intraplacental T2-dark bands are also present (arrow). **(E)** Sagittal T2-weighted image shows a network of flow voids (arrows) related to abnormal vascularization of the placental bed. The patient delivered by cesarean section, and hysterectomy was performed. Pathologic evaluation of the placenta revealed myoinvasion with placenta extending within 0.2 cm of the serosal surface, pathologic grade 3A (not shown).

at pathologic examination, there is no true villous invasion into the serosa or residual myometrium.

Bladder Wall Interruption.—Focal interruption or irregularity of the normal T2-hypointense bladder wall is concerning for bladder wall involvement. The bladder should be moderately distended for optimal evaluation. Direct nodular placental invasion into the bladder is diagnostic of placenta percreta but is rarely seen (25,48). Similarly, the presence of bladder tenting is highly associated with placenta percreta, with sensitivity of 52.6% and specificity of 90.2% (48). The bladder vessel sign and serosal vessel sign—which refer to flow voids in the bladder wall and serosa or vesicouterine space—are also highly suspicious for bladder wall involvement (25) (Figs 9C, 10D).

Focal Exophytic Mass.—Focal exophytic mass refers to invasion of placental tissue into the myometrium, breaking through the T2-hypointense uterine serosal margin, with variable extension beyond the serosal surface (Fig 3B). This sign is most often seen along the anterior aspect of the uterus toward the bladder or into the parametrium. This finding is highly specific for placenta percreta, with a recent meta-analysis demonstrating specificity of 98.9% when it extends toward the bladder, but it has low sensitivity (69.2%) overall for PAS disorders, as it is not seen in placenta accreta or placenta increta (48).

Loss of T2-hypointense Retroplacental Line.—Focal interruption or diffuse loss of the T2-hypointense placental–inner myometrial interface can be seen in PAS disorders (64) (Figs 5C, 5D, 8C, 9C, 9D, 10B, 10C). It is often seen in conjunction with myometrial thinning and correlates with loss of the retroplacental clear zone at sonographic evaluation. As with myometrial thinning, this line may be difficult to visualize in late gestation and should be interpreted in conjunction with other findings.

Abnormal Vascularization of the Placental Bed.—The retroplacental bed consists of normal vessels, decidua, and adjacent myometrium. Owing to vascular placental changes in PAS disorders, these vessels lose their uniform appearance of T2-hypointense flow voids and become heterogeneous in size, with disruption of the uteroplacental interface (Figs 5E, 7C, 7D). This network of abnormal vessels may extend into the

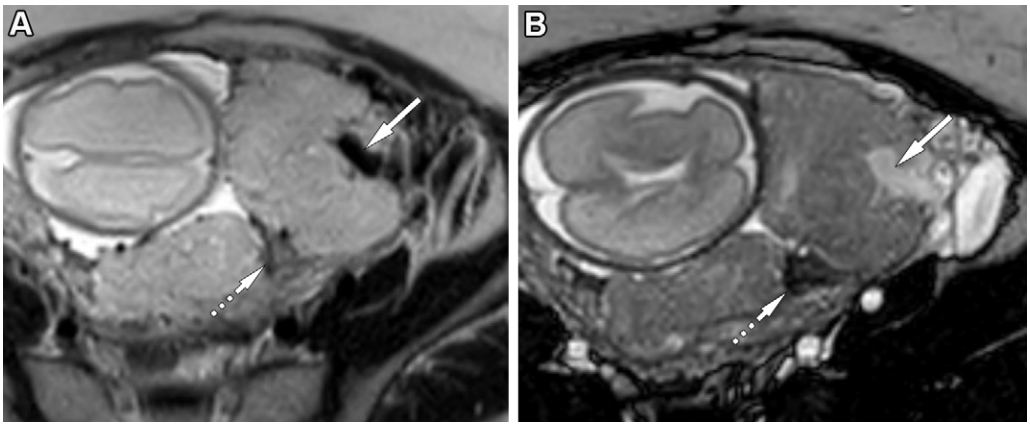

Figure 6. Intraplacental dark bands in a 35-year-old patient at 26 weeks gestation with a history of placenta previa. **(A)** Axial T2-weighted image shows an intraplacental irregular T2-dark band (dashed arrow) extending from the maternal surface of the placenta and traversing the entire width of the placental tissue. Note the abnormal intraplacental vascularity anteriorly with the flow void of a large vessel (solid arrow), which can mimic an intraplacental dark band. **(B)** Axial SSFP image allows further distinction of the T2-hyperintense vessel (solid arrow) from the T2-dark band (dashed arrow), which is hypointense. Bands will remain hypointense on SSFP images.

Figure 7. Myoinvasive PAS disorder in a 31-year-old patient who presented at 32 weeks gestation with vaginal bleeding. **(A, B)** Long-axis gray-scale **(A)** and color Doppler **(B)** transabdominal US images of the placenta show thinned myometrium over the anterior placenta and placental bulge with associated uterovesical interface hypervascularity (arrow). **(C)** Sagittal T2-weighted image through the placenta shows placenta previa with widening of the lower uterine segment. Note the intraplacental dark bands (arrowhead), abnormal vascularization of the placental bed (dashed arrow), and anterior placental bulge with associated myometrial thinning (solid arrow). **(D)** Duplicated sagittal T2-weighted image outlined with the contour of the placental bulge anteriorly (black line) and the normal placental-myometrial interface posteriorly (white line). Normal myometrium (white arrowheads) is seen both anteriorly above the area of the bulge and posteriorly with vascular myometrial engorgement. Black arrowhead = intraplacental dark bands, dashed arrow = abnormal vascularization of the placental bed, solid arrow = anterior placental bulge with associated myometrial thinning. **(E)** Axial T2-weighted image shows myometrial thinning on the anterior placental margin corresponding to the bulge seen on the sagittal image (solid arrow). Note the normal posterior myometrium with a trilaminar appearance (dashed arrow) and myometrial engorgement (arrowheads). Myometrial engorgement should not be mistaken for a placental bulge in this region. DWI (not shown) can be helpful for this delineation (Fig 4). The patient delivered via cesarean section at 35 weeks gestation, and hysterectomy was performed. Pathologic evaluation revealed deep myoinvasion approximately 0.1 cm from the anterior serosal surface, pathologic grade 3A (not shown).

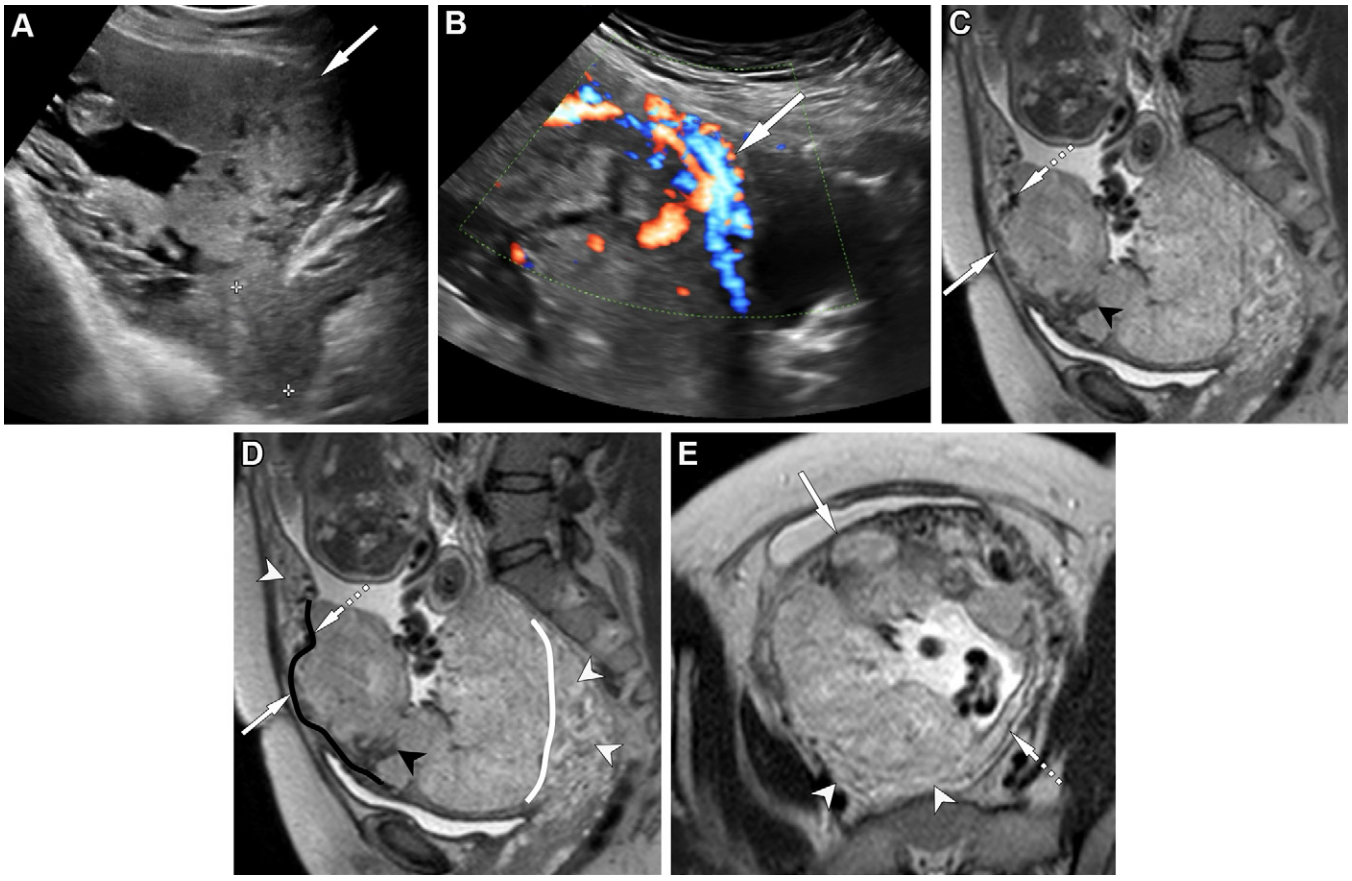

myometrium and course along the serosa, appearing hypertrophied around the bladder, uterus, and vagina.

The presence of vessels within the vesicouterine space is highly suspicious for bladder wall involvement. Similarly, vessels extending from the uterine surface into the parametrial fat—the parametrial vessel sign—has specificity of 86.8% for PAS disorders and is an independent predictor of parametrial invasion (25). Normal increase in periuterine

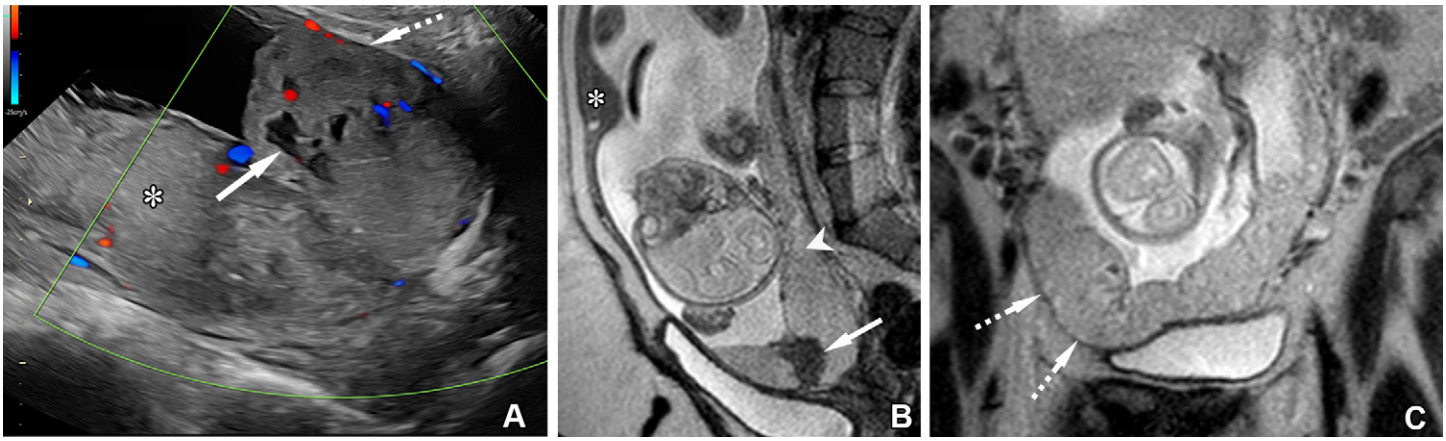

Figure 8. Myoinvasive PAS disorder in a 35-year-old patient at 27 weeks gestation with a history of three prior cesarean sections. **(A)** Long-axis US image shows complete placenta previa, with a largely posterior placenta (*) with anterior lower uterine segment myometrial thinning (dashed arrow) and placental lacunae (solid arrow). **(B, C)** Sagittal **(B)** and coronal **(C)** T2-weighted images show a largely posterior placenta (arrowhead in **B**), with a T2-dark intraplacental band (arrow in **B**) anterior to the cervix and placental bulge, myometrial thinning, and loss of the T2-hypointense retroplacental line in the right lower uterine segment (arrows in **C**). Note the normal anterior myometrial contraction (* in **B**). The patient delivered at 33 weeks via cesarean section. Intraoperatively, there was invasion beyond the serosa, with bilateral parametrial involvement extending to the pelvic sidewall on the right. The patient was managed with a delayed hysterectomy approach.

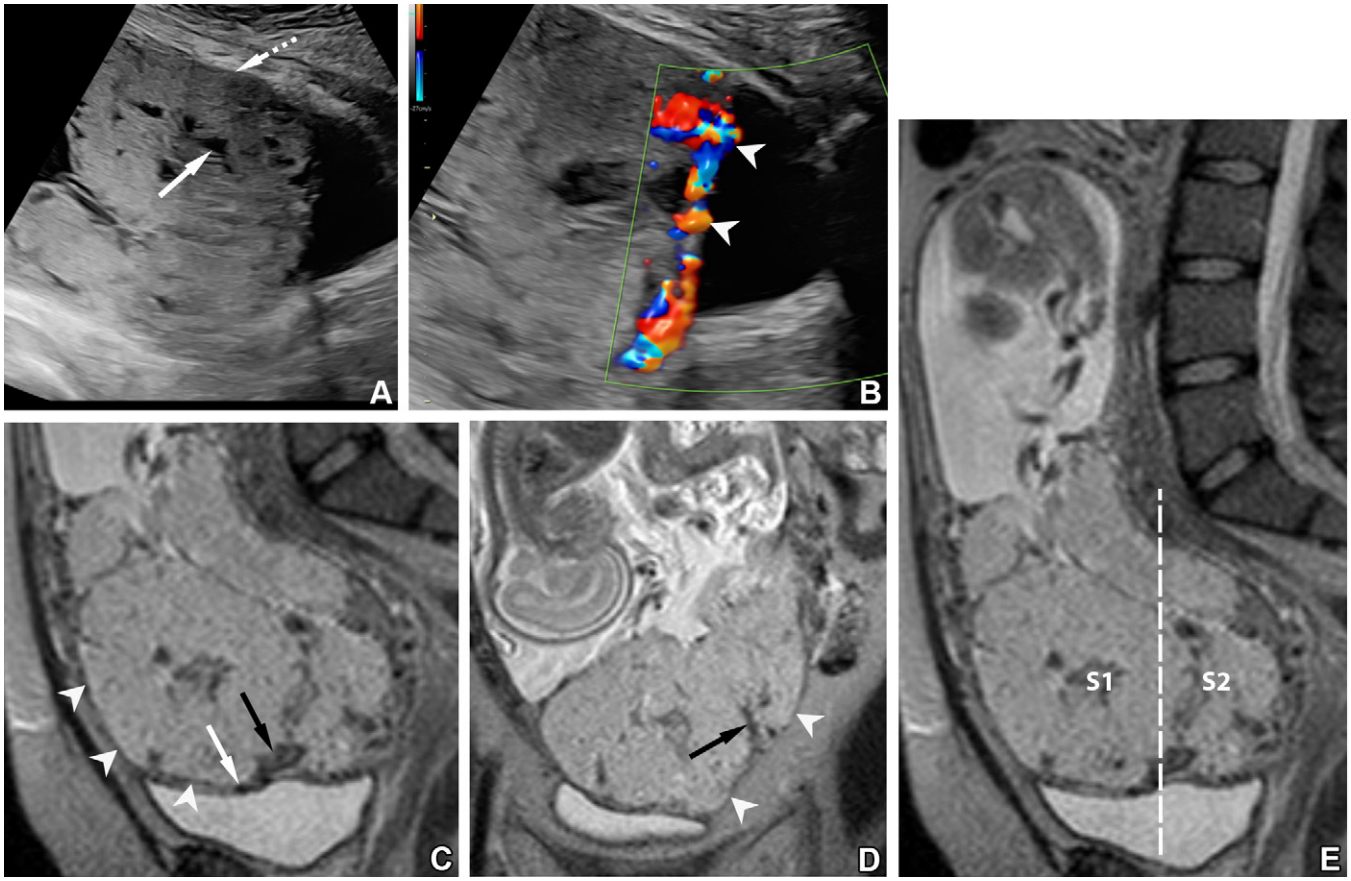

Figure 9. Myoinvasive PAS disorder in a 23-year-old patient with vaginal bleeding and preterm premature rupture of membranes (PPROM) at 20 weeks gestation. **(A, B)** Long-axis gray-scale **(A)** and color Doppler **(B)** US images show multiple placental lacunae (solid arrow in **A**), with overlying myometrial thinning along the anterior lower uterine segment (dashed arrow in **A**) and marked uterovesical hypervascularity (arrowheads in **B**). **(C, D)** Sagittal **(C)** and coronal **(D)** T2-weighted images show a heterogeneous placenta with focal left anterolateral bulge and anterior myometrial thinning with loss of the T2-hypointense retroplacental line (arrowheads). Note the intraplacental T2-dark bands (black arrow), as well as a few flow voids at the placental-bladder interface (white arrow in **C**). **(E)** Duplicated sagittal full-field-of-view image with a dotted line delineating topographic sectors S1 and S2. The S1 sector includes the uterine body, while the S2 sector includes the lower uterine segment, cervix, and upper vagina. Note the widening of the lower uterine segment and the hourglass configuration of the uterus. The patient was managed with gravid hysterectomy (due to previability). Intraoperative and cystoscopic findings were suspicious for invasion into the muscularis layer of the bladder dome, which required a 1-cm cystostomy. However, final pathologic evaluation demonstrated only serosal involvement, pathologic Grade 3D (not shown).

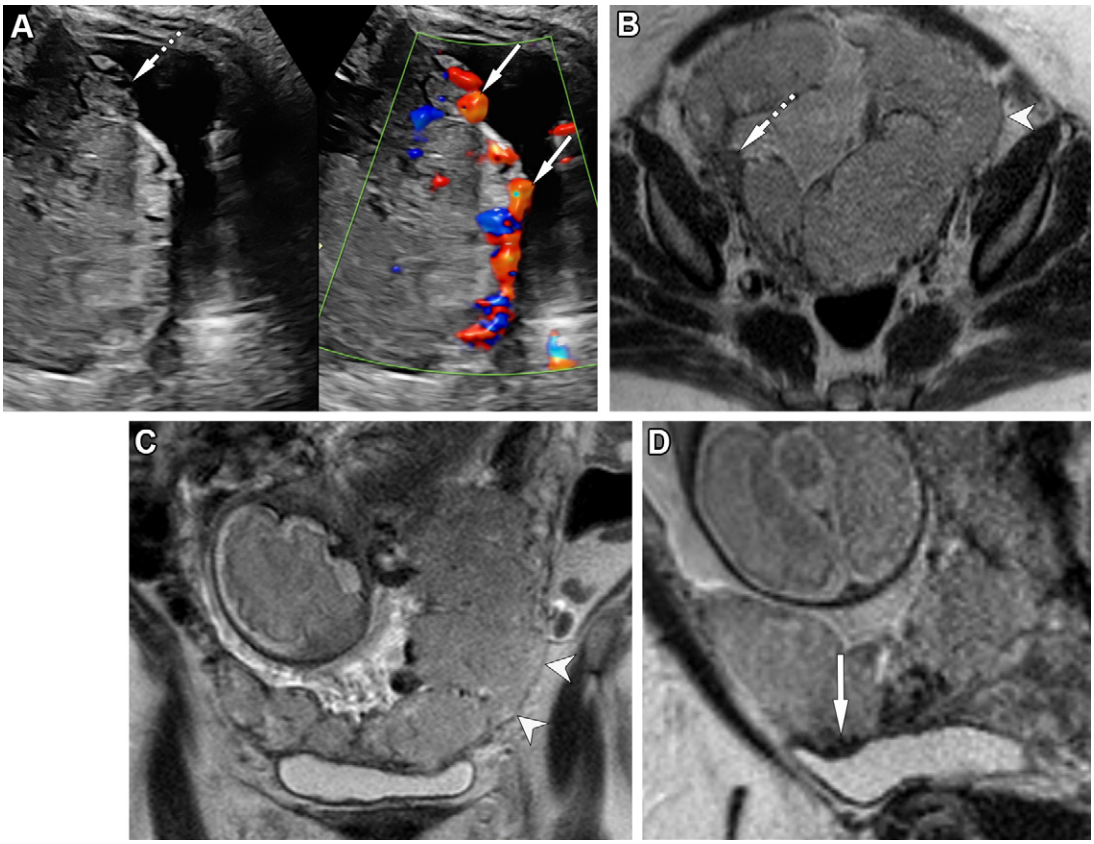

Figure 10. Myoinvasive PAS disorder in a 32-year-old patient with a history of three prior cesarean sections. **(A)** Transverse split-screen gray-scale and color Doppler transabdominal US images of the uterovesical junction show an exophytic mass (dashed arrow) and several vascular structures in the bladder wall (solid arrows), representing uterovesical hypervascularity and bridging vessels. **(B–D)** Axial **(B)**, coronal **(C)**, and sagittal **(D)** MR images at 31 weeks gestation show a T2-dark band (arrow in **B**), myometrial thinning, placental bulge, and loss of the T2-hypointense retroplacental line along the left lateral placental margin (arrowheads in **B** and **C**), and several flow voids along the bladder-placental interface (arrow in **D**), known as the bladder vessel sign. The patient delivered at 35 weeks gestation via cesarean section. Intraoperative cystoscopy revealed bulging tortuous vessels. Surgical intraoperative findings included placenta extending to the bladder serosa with concern for muscularis involvement at the trigone. The patient was managed with a delayed hysterectomy approach.

vascularity late in gestation is a known pitfall, emphasizing the need for the presence of other signs to support the diagnosis of PAS disorder.

Additional Features.—Additional imaging features are also discussed in the consensus statement as predictors of PAS disorders; however, these features did not meet consensus and were categorized as uncertain (27). Inability to reach consensus was attributed to subjective nature, interreader variability, and overlap with expected evolving placental features in late gestation. These additional features include the following four features: placental heterogeneity, asymmetric thickening or shape of the placenta, placental ischemic infarction, and abnormal intraplacental vascularity (Table 3).

While placental heterogeneity did not meet consensus, this finding has been described in the literature as having good sensitivity and specificity for PAS disorders of 75% and 65.9% for placenta accreta, 81.8% and 71.1% for placenta increta, and 73.9% and 62.7% for placenta percreta, respectively (48). Abnormal intraplacental vascularity has been associated with PAS disorders with lower sensitivities than the other uncertain features (46%–53.8%) (48). Vessel enlargement was defined as greater than 6 mm in diameter when first described and thought to be maternal in origin, originating from myometrium at the invasive margin (65). However, recent literature suggests that vessels that are fetal in origin, measuring greater than 3 mm at MRI, extending from the cord or chorionic or subchorionic placental surface, and traveling deep into the placenta are associated with placenta percreta and peripartum complications (21,66,67).

Prognostic Considerations of MRI Features.—Specific MRI features or combinations of features for predicting severe disease or poor maternal outcome are being increasingly investigated. Increasing volume of bands is associated with increased depth of invasion (19). Chen et al (68) found that placental bulge and uterine serosal hypervascularity are independently associated with placenta percreta. Thiravit et al (61) suggested that uterine bulge is an independent predictor of myoinvasive PAS disorder, and Bourgioti et al (66) suggested that fetal intraplacental vessel size greater than 3 mm is associated with peripartum complications, including massive hemorrhage.

A study by Bourgioti et al (25) demonstrated that specific features (intraplacental dark bands, myometrial disruption, uterine bulge, and hypervascularity at the uteroplacental interface) are associated with poor clinical outcome for both patient and fetus and that an increasing number of MRI features allow prediction of the peripartum course. They found that the presence of three or more features was associated with complicated delivery, and the presence of six or more features was associated with massive bleeding, hysterectomy, or extensive bladder repair.

Advanced Imaging Techniques.—DWI may be an adjunct tool in diagnosis of PAS disorders. While DWI has not been shown to increase diagnostic accuracy compared with conventional sequences, it may allow better delineation of the myometrial-placental interface compared with T2-weighted imaging (55,69) (Fig 4). Additional advantages of DWI include minimal motion artifact and the ability for fusion with $b = 0$ sec/mm^2 images, where signal intensity between the

Figure 11. Myoinvasive PAS disorder with a delayed hysterectomy approach in a 31-year-old patient with a history of two prior cesarean sections. US at 25 weeks gestation showed placenta previa with marked myometrial thinning and a large right focal placental bulge (not shown). MRI was performed at 28 weeks gestation. **(A, B)** Sagittal **(A)** and axial **(B)** T2-weighted images show widening of the lower uterine segment and a T2-dark area of placental thinning (arrow in **A**) due to focal placental infarction. Incidentally noted is a normal myometrial contraction (∗ in **A**). There is myometrial thinning anterolaterally on the right (solid arrow in **B**) at the site of the placental bulge and a T2-dark intraplacental band (dashed arrow in **B**). The patient underwent cesarean delivery at 34 weeks gestation. Intraoperatively, there was extension of placenta into the right parametrium and pelvic sidewall with adherence to the bladder. The hysterotomy was closed, and placental tissue was left in situ. Serial MRI was performed to evaluate for placental involution. **(C, D)** Sagittal T2-weighted image **(C)** and contrast-enhanced T1-weighted image **(D)** with fat suppression 1 month after delivery show large residual placental tissue with diffuse enhancement (arrows). **(E, F)** Sagittal T2-weighted image **(E)** and contrast-enhanced T1-weighted image **(F)** with fat suppression 2 months after delivery show decreasing residual placental tissue with a few focal areas of enhancement (arrows). Delayed hysterectomy was performed 8 weeks after delivery without any complications.

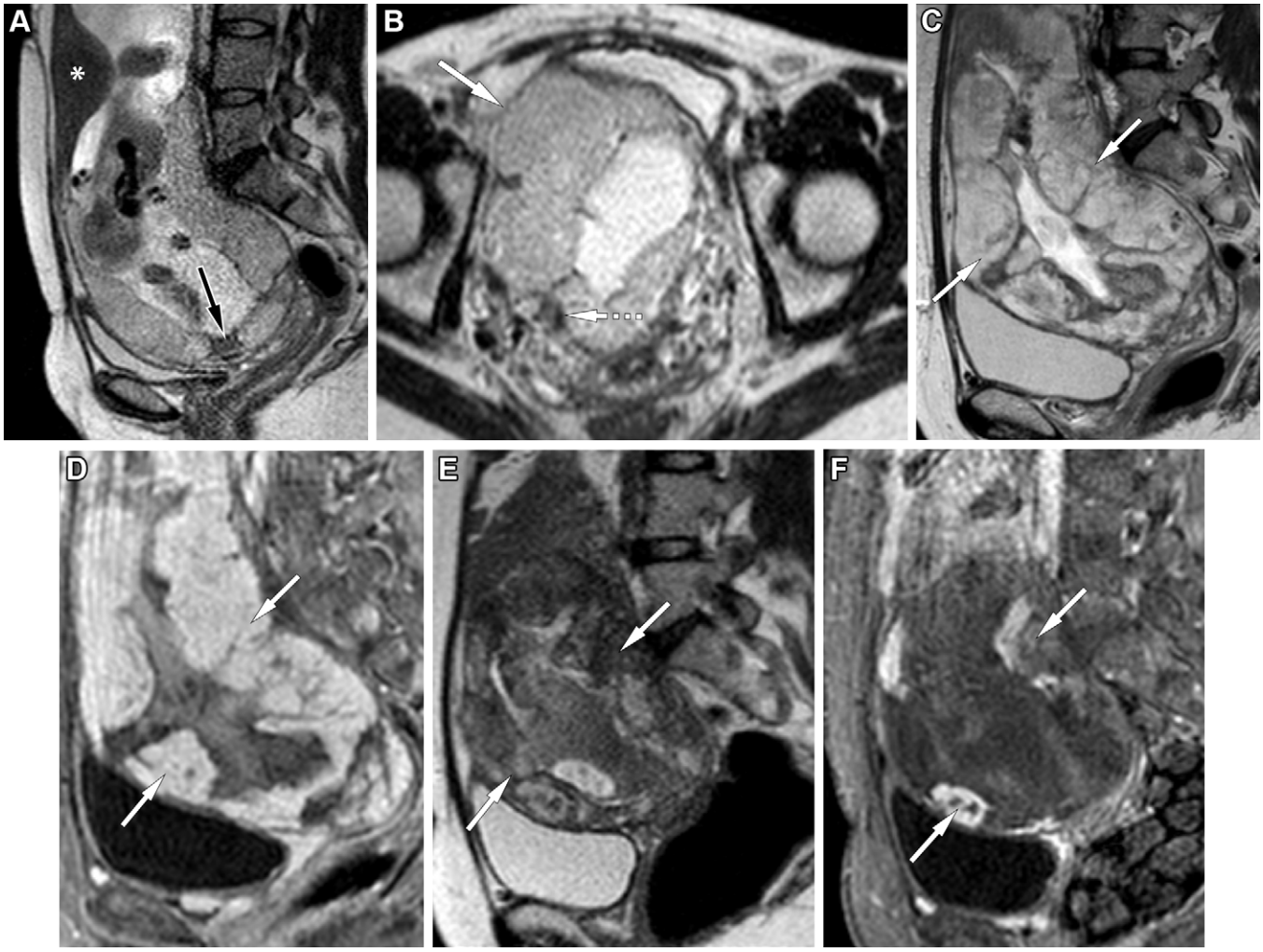

parametrial fat and myometrial margin is greatest. A small study by Morita et al (69) describes how this technique would allow measurement of myometrial thickness and identification of areas of focal myometrial thinning.

MRI-derived textural analysis may also provide quantifiable data for the subjective feature of placental heterogeneity, which would presumably correlate with underlying histologic abnormalities. Several models in the literature demonstrate statistical significance between normal and abnormal placenta, good accuracy for diagnosis of PAS disorders, and predictive capabilities for those PAS disorder cases requiring cesarean section (70–73).

Structured Reporting.—A structured reporting template is provided in the joint consensus statement (27). This includes key clinical features such as maternal age, gestational age, number of prior cesarean sections, presence of placenta previa, and pertinent US findings prompting MRI. The presence of placenta previa and the exact location of the placenta relative to the patient's anatomy are important for the type and location of the skin incision and the surgical approach for delivery.

The presence or absence of the 11 imaging features (seven recommended and four uncertain), suspected depth and location of myoinvasion, and extrauterine extension should be included in the radiology report. Involvement of critical structures—such as the bladder, bowel, parametrium, pelvic sidewall, ureters, and abdominal wall—and the relationship to major vessels, especially the internal iliac vasculature, are critical to the surgical approach and multidisciplinary surgical team engagement for delivery. Additionally, invasion of

Table 3: MRI Features Categorized as Uncertain

MRI Feature Categorized as Uncertain	Definition
Placental heterogeneity	Heterogeneous signal intensity on both T1- and T2-weighted images, related to a combination of underlying bands, abnormal intraplacental vascularity, and lacunae (Fig 12A)
Asymmetric thickening or shape of placenta	Thickening at the area of suspected PAS disorder, which is often located over the internal cervical os, often with corresponding increased placental heterogeneity (Fig 12A)
Placental ischemic infarction	Areas of asymmetric placental thinning due to repeated infarction (Fig 11A) Pitfall: areas of peripheral infarct can be seen in normal placenta late in gestation, especially in the setting of underlying placental insufficiency
Abnormal intraplacental vascularity	Abnormal vessels or tortuous enlarged flow voids within the placental mass, particularly those vessels located away from the site of cord insertion (Fig 6)

the cervix—as evidenced by protrusion of the placenta into the internal cervical os—should be described, as supracervical hysterectomy would be avoided in this setting.

The topography of invasion can be described using an anatomic classification of anterior placental invasion described in the surgical literature, which divides the uterus into two sectors—S1 and S2—on the basis of uterine vascular supply (60). At MRI, the delineation is made by drawing a line perpendicular to the middle of the posterior bladder wall. The upper sector bordering the upper bladder wall is termed *S1* and corresponds to the uterine body. The lower sector bordering the lower bladder wall is termed *S2* and includes the lower uterine segment, cervix, and upper vagina (Fig 9E). The clinical relevance of this anatomic delineation is the association of increased maternal morbidity with S2 invasion, prompting surgical and vascular control measures to decrease the risk of surgical complications (74).

Patient Management

Antenatal diagnosis of PAS disorders and management by a multidisciplinary team with clinical expertise is key to optimal outcomes for affected patients (16,75,76). Maternal morbidity and mortality are predominantly due to massive hemorrhage, leading to complications such as disseminated intravascular coagulation (DIC), coagulopathy, multiorgan failure, and potentially death. Multidisciplinary team preparedness includes careful antenatal care planning by the maternal-fetal medicine specialist, radiologic expertise for diagnosis and presurgical planning, surgical expertise allowing for both the complexity of PAS disorder pelvic surgery and potential complications (ureter, bladder, or bowel injury), as well as prompt availability of resources for massive blood transfusion, interventional radiology embolization, and adult and neonatal intensive care unit (ICU) care should they be needed (16).

Scheduled nonemergent cesarean hysterectomy is the management of choice per the American College of Obstetricians and Gynecologists (ACOG) and Society for Maternal-Fetal Medicine (SMFM) and is chosen in the vast majority of patients with PAS disorders (11). This includes delivery of the fetus followed by immediate hysterectomy without attempt to separate the invasive placental tissue from the uterus, which could result in massive hemorrhage. The timing of delivery for cases of PAS disorders is between 34 and 36 weeks gestation.

Importantly, imaging guides management. Localization of the placenta relative to the patient's anatomy determines the location of the skin and hysterotomy incision and the surgical approach for delivery. The depth and topography of invasion are critical to surgical planning, identifying areas of difficult devascularization and dissection, and may impact use of a range of adjuvant therapies, such as pre- or intraoperative uterine vessel embolization, vessel ligation, arterial balloon placement, ureteral catheter placement, and medication therapy (16).

Cesarean hysterectomy remains associated with high morbidity (40%–50%) and mortality (up to 7%) owing to damage to adjacent organs and pelvic vasculature (5). Delayed hysterectomy is an alternative surgical management strategy that may be considered when severe myoinvasion or lateral extension of placental bulk makes immediate cesarean hysterectomy difficult. The uterus and placenta are left in situ after cesarean delivery with repair of the hysterotomy site, and planned elective hysterectomy is performed 3–12 weeks later (16,77,78).

Additional conservative or expectant management approaches for PAS disorders include those attempting to avoid hysterectomy altogether and include a combination of surgical techniques and leaving the placenta in situ (5). These approaches allow uterine blood flow to decrease, with resultant progressive involution of the placenta and regression from surrounding pelvic structures in the postpartum period (5). Postpartum MRI may be performed to assess interval involution of the placenta left in situ and any additional associated vascularity and topography of the residual placental mass (Figs 11, 12).

The common goal in these alternative approaches is to decrease the risk of severe maternal morbidity during cesarean delivery, with the caveat of increased postpartum risks of coagulopathy, hemorrhage, and sepsis. Overall, this wide range and combination of therapeutic strategies limits the ability to determine a single "best" management approach. The option of conservative or expectant management is considered only in carefully selected cases in conjunction with institutional experience and expertise (Fig 13) (5,16,77,79–82).

Conclusion

PAS disorders are a major cause of maternal morbidity and mortality, with rising prevalence thought to be related to the

Figure 12. Myoinvasive PAS disorder in a 36-year-old woman with a history of prior dilation and curettage (D&C) and uterine laser surgery for polyp and fibroid removal. This patient was inadvertently managed expectantly. MRI was performed at 23 weeks gestation owing to concern for PAS disorder in an outside hospital after US evaluation (not shown). **(A)** Sagittal T2-weighted image shows placenta previa with asymmetric thickening and shape of the placenta. Note the thinned myometrium anteriorly and posteriorly (arrowheads). There is placental heterogeneity (arrows) overlying the cervix with areas of thinning, reflecting a combination of placental infarcts and T2-dark bands. The patient delivered at 34 weeks via cesarean section. Intraoperatively, there was circumferential deep placental invasion of the myometrium extending into the bilateral parametrium, adherent to the bladder. The uterus and placenta were left in situ for gradual involution. **(B, C)** Sagittal T2-weighted image **(B)** and contrast-enhanced T1-weighted image with fat suppression **(C)** 6 weeks after delivery show significant T2-heterogeneous residual placental tissue with diffuse enhancement (arrows). The patient was planned to undergo a delayed hysterectomy approach but was lost to follow-up. **(D, E)** Sagittal T2-weighted image **(D)** and contrast-enhanced T1-weighted image with fat suppression **(E)** 7 months after delivery show a large amount of residual T2-heterogeneous placental tissue without discernible enhancement due to necrosis (arrows), with thin overlying intact serosa. The patient was again lost to follow-up and presented 3 years after delivery, undergoing evaluation in an attempt to conceive again. MRI was performed for evaluation of the uterus. **(F, G)** Sagittal T2-weighted image **(F)** and subtraction contrast-enhanced T1-weighted image with fat suppression **(G)** show scarring and thinning of the lower uterine segment at the cesarean niche and a posterior isthmocele (arrow) containing T2 mildly hyperintense blood products (with intrinsic hyperintensity at T1-weighted imaging, not shown) without any enhancement.

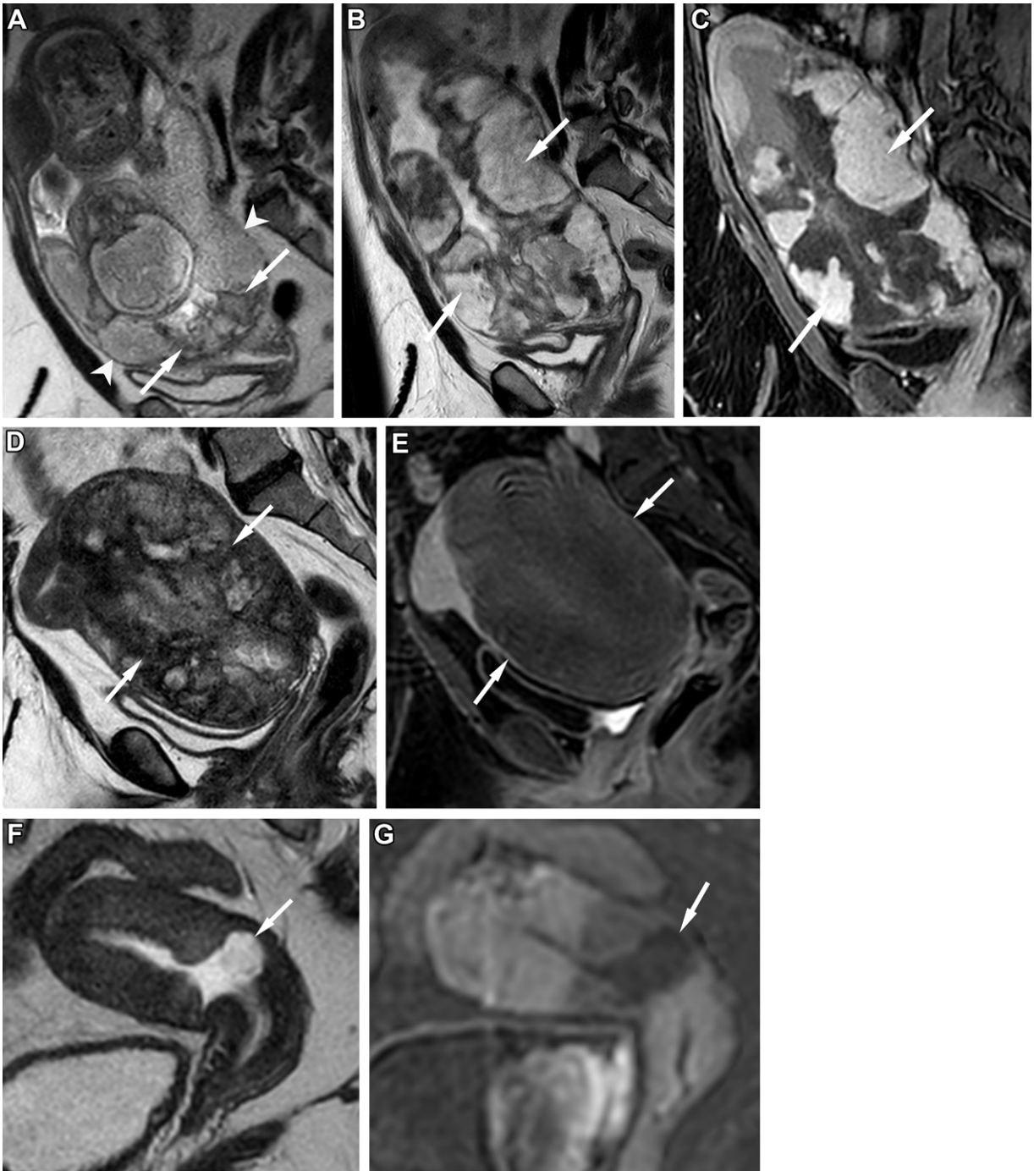

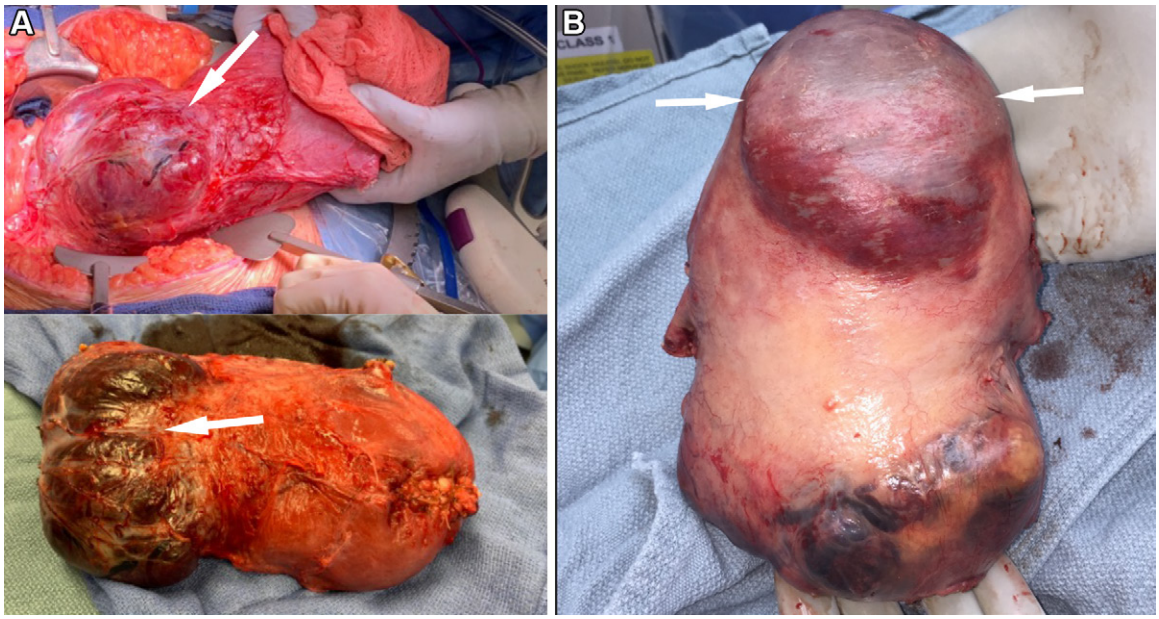

Figure 13. **(A)** Intraoperative (top) and specimen (bottom) photographs of the uterus in a patient at 35 weeks gestation at the time of delivery show severe myoinvasive PAS disorder. Placental bulk (arrow) is located in the midline lower uterine segment with placental bulge and increased vascularity within the serosa. In this case, since the lateral walls were free from extension and the bladder was not adherent to the uterus, cesarean hysterectomy was performed without complication. Estimated blood loss was 300 mL. **(B)** Photograph of a delayed hysterectomy specimen in another patient 8 weeks after cesarean delivery show significant regression of vascularity and placental tissue in the anterior and lateral lower uterine segment (arrows).

increased rate of cesarean delivery. Accurate antenatal diagnosis and a multidisciplinary approach are key to optimal management and improved outcome for these patients. US is the first-line examination, and MRI serves a complementary role, with particular value in equivocal US diagnoses and evaluating extent of invasion for surgical planning in the most severe cases.

The SAR-ESUR joint consensus statement provides seven major MRI features recommended for use in diagnosis of PAS disorders. While no single feature is diagnostic of PAS disorder, the combination of features and the presence of multiple features in the context of elevated clinical risk increase the likelihood of underlying PAS disorder. Familiarity with the spectrum of MRI findings of PAS disorders and deeper understanding of the clinical relevance of each sign provide the radiologist with the tools needed to more accurately diagnose this disease and make a greater impact on patient care.

Author affiliations.—From the Department of Radiology and Radiological Sciences (K.K.P.L, V.B.P., C.H.P., M.M.) and Department of Obstetrics and Gynecology (L.C.Z.), Vanderbilt University Medical Center, 1161 21st Ave South, Nashville, TN 37232; and Department of Diagnostic Imaging and Radiology, University of Louisville, Louisville, Ky (J.M.O.). Presented as an education exhibit at the 2021 RSNA Annual Meeting. Received April 18, 2022; revision requested August 26 and received September 7; accepted September 9. **Address correspondence to** K.K.P.L. (email: *Krupa.k.patel-lippmann@vumc.org*).

Disclosures of conflicts of interest.—**C.H.P.** Honorarium for presenting a lecture to the Sonographer Society of South Florida; Deputy Editor for Obstetric and Gynecologic Radiology, RSNA Case Collection. **M.M.** Editor, RSNA Case Collection. All other authors, the editor, and the reviewers have disclosed no relevant relationships.

References

1. Jauniaux E, Jurkovic D. Placenta accreta: pathogenesis of a 20th century iatrogenic uterine disease. Placenta 2012;33(4):244–251.
2. Matsuzaki S, Mandelbaum RS, Sangara RN, et al. Trends, characteristics, and outcomes of placenta accreta spectrum: a national study in the United States. Am J Obstet Gynecol 2021;225(5):534.e1–534.e38.
3. Jauniaux E, Bunce C, Grønbeck L, Langhoff-Roos J. Prevalence and main outcomes of placenta accreta spectrum: a systematic review and meta-analysis. Am J Obstet Gynecol 2019;221(3):208–218.
4. Fonseca A, Ayres de Campos D. Maternal morbidity and mortality due to placenta accreta spectrum disorders. Best Pract Res Clin Obstet Gynaecol 2021;72:84–91.
5. Sentilhes L, Kayem G, Chandraharan E, Palacios-Jaraquemada J, Jauniaux E; FIGO Placenta Accreta Diagnosis and Management Expert Consensus Panel. FIGO consensus guidelines on placenta accreta spectrum disorders: conservative management. Int J Gynaecol Obstet 2018;140(3):291–298.
6. Jauniaux E, Chantraine F, Silver RM, Langhoff-Roos J; FIGO Placenta Accreta Diagnosis and Management Expert Consensus Panel. FIGO consensus guidelines on placenta accreta spectrum disorders: epidemiology. Int J Gynaecol Obstet 2018;140(3):265–273.
7. Silver RM, Landon MB, Rouse DJ, et al. Maternal morbidity associated with multiple repeat cesarean deliveries. Obstet Gynecol 2006;107(6):1226–1232.
8. Klar M, Michels KB. Cesarean section and placental disorders in subsequent pregnancies: a meta-analysis. J Perinat Med 2014;42(5):571–583.
9. FastStats. 2021. https://www.cdc.gov/nchs/fastats/delivery.htm. Accessed January 19, 2022.
10. Wu S, Kocherginsky M, Hibbard JU. Abnormal placentation: twenty-year analysis. Am J Obstet Gynecol 2005;192(5):1458–1461.
11. Society of Gynecologic Oncology; American College of Obstetricians and Gynecologists and the Society for Maternal–Fetal Medicine; Cahill AG, et al. Placenta Accreta Spectrum. Am J Obstet Gynecol 2018;219(6):B2–B16.
12. Jauniaux E, Ayres-de-Campos D; FIGO Placenta Accreta Diagnosis and Management Expert Consensus Panel. FIGO consensus guidelines on placenta accreta spectrum disorders: introduction. Int J Gynaecol Obstet 2018;140(3):261–264.
13. Jauniaux E, Hecht JL, Elbarmelgy RA, Elbarmelgy RM, Thabet MM, Hussein AM. Searching for placenta percreta: a prospective cohort and systematic review of case reports. Am J Obstet Gynecol 2022;226(6):837.e1–837.e13.

14. Jauniaux E, Jurkovic D, Hussein AM, Burton GJ. New insights into the etiopathology of placenta accreta spectrum. Am J Obstet Gynecol 2022;227(3):384–391.
15. Jauniaux E, Ayres-de-Campos D, Langhoff-Roos J, Fox KA, Collins S; FIGO Placenta Accreta Diagnosis and Management Expert Consensus Panel. FIGO classification for the clinical diagnosis of placenta accreta spectrum disorders. Int J Gynaecol Obstet 2019;146(1):20–24.
16. Allen L, Jauniaux E, Hobson S, Papillon-Smith J, Belfort MA; FIGO Placenta Accreta Diagnosis and Management Expert Consensus Panel. FIGO consensus guidelines on placenta accreta spectrum disorders: nonconservative surgical management. Int J Gynaecol Obstet 2018;140(3):281–290.
17. Jauniaux E, Bhide A, Kennedy A, Woodward P, Hubinont C, Collins S; FIGO Placenta Accreta Diagnosis and Management Expert Consensus Panel. FIGO consensus guidelines on placenta accreta spectrum disorders: prenatal diagnosis and screening. Int J Gynaecol Obstet 2018;140(3):274–280.
18. Hecht JL, Baergen R, Ernst LM, et al. Classification and reporting guidelines for the pathology diagnosis of placenta accreta spectrum (PAS) disorders: recommendations from an expert panel. Mod Pathol 2020;33(12):2382–2396.
19. Lim PS, Greenberg M, Edelson MI, Bell KA, Edmonds PR, Mackey AM. Utility of ultrasound and MRI in prenatal diagnosis of placenta accreta: a pilot study. AJR Am J Roentgenol 2011;197(6):1506–1513.
20. Lax A, Prince MR, Mennitt KW, Schwebach JR, Budorick NE. The value of specific MRI features in the evaluation of suspected placental invasion. Magn Reson Imaging 2007;25(1):87–93.
21. Derman AY, Nikac V, Haberman S, Zelenko N, Opsha O, Flyer M. MRI of placenta accreta: a new imaging perspective. AJR Am J Roentgenol 2011;197(6):1514–1521.
22. Leyendecker JR, DuBose M, Hosseinzadeh K, et al. MRI of pregnancy-related issues: abnormal placentation. AJR Am J Roentgenol 2012;198(2):311–320.
23. Allen BC, Leyendecker JR. Placental evaluation with magnetic resonance. Radiol Clin North Am 2013;51(6):955–966.
24. Teo TH, Law YM, Tay KH, Tan BS, Cheah FK. Use of magnetic resonance imaging in evaluation of placental invasion. Clin Radiol 2009;64(5):511–516.
25. Bourgioti C, Zafeiropoulou K, Fotopoulos S, et al. MRI Features Predictive of Invasive Placenta with Extrauterine Spread in High-Risk Gravid Patients: A Prospective Evaluation. AJR Am J Roentgenol 2018;211(3):701–711.
26. Morel O, Collins SL, Uzan-Augui J, et al. A proposal for standardized magnetic resonance imaging (MRI) descriptors of abnormally invasive placenta (AIP): from the International Society for AIP. Diagn Interv Imaging 2019;100(6):319–325.
27. Jha P, Põder L, Bourgioti C, et al. Society of Abdominal Radiology (SAR) and European Society of Urogenital Radiology (ESUR) joint consensus statement for MR imaging of placenta accreta spectrum disorders. Eur Radiol 2020;30(5):2604–2615.
28. Huppertz B. The anatomy of the normal placenta. J Clin Pathol 2008;61(12):1296–1302.
29. Gauster M, Moser G, Wernitznig S, Kupper N, Huppertz B. Early human trophoblast development: from morphology to function. Cell Mol Life Sci 2022;79(6):345.
30. Wamaitha SE, Niakan KK. Human Pre-gastrulation Development. Curr Top Dev Biol 2018;128:295–338.
31. Kellow ZS, Feldstein VA. Ultrasound of the placenta and umbilical cord: a review. Ultrasound Q 2011;27(3):187–197.
32. Kanne JP, Lalani TA, Fligner CL. The placenta revisited: radiologic-pathologic correlation. Curr Probl Diagn Radiol 2005;34(6):238–255.
33. Blaicher W, Brugger PC, Mittermayer C, et al. Magnetic resonance imaging of the normal placenta. Eur J Radiol 2006;57(2):256–260.
34. Kim JA, Narra VR. Magnetic resonance imaging with true fast imaging with steady-state precession and half-Fourier acquisition single-shot turbo spin-echo sequences in cases of suspected placenta accreta. Acta Radiol 2004;45(6):692–698.
35. De Oliveira Carniello M, Oliveira Brito LG, Sarian LO, Bennini JR. Diagnosis of placenta accreta spectrum in high-risk women using ultrasonography or magnetic resonance imaging: systematic review to compare accuracy of tests. Ultrasound Obstet Gynecol 2022;59(4):428–436.
36. D'Antonio F, Iacovella C, Palacios-Jaraquemada J, Bruno CH, Manzoli L, Bhide A. Prenatal identification of invasive placentation using magnetic resonance imaging: systematic review and meta-analysis. Ultrasound Obstet Gynecol 2014;44(1):8–16.
37. Pagani G, Cali G, Acharya G, et al. Diagnostic accuracy of ultrasound in detecting the severity of abnormally invasive placentation: a systematic review and meta-analysis. Acta Obstet Gynecol Scand 2018;97(1):25–37.
38. Timor-Tritsch IE, Monteagudo A, Cali G, El Refaey H, Kaelin Agten A, Arslan AA. Easy sonographic differential diagnosis between intrauterine pregnancy and cesarean delivery scar pregnancy in the early first trimester. Am J Obstet Gynecol 2016;215(2):225.e1–225.e7.
39. Panaiotova J, Tokunaka M, Krajewska K, Zosmer N, Nicolaides KH. Screening for morbidly adherent placenta in early pregnancy. Ultrasound Obstet Gynecol 2019;53(1):101–106.
40. Flores-Mendoza H, Windrim RC, Kingdom JC, Hobson SR. Improving Early Pregnancy Screening for Placenta Accreta Spectrum: Retrospective Analysis of Early Screening Candidates by Risk Assessment in Canada. J Obstet Gynaecol Can 2022;44(6):704–706.
41. Collins SL, Ashcroft A, Braun T, et al. Proposal for standardized ultrasound descriptors of abnormally invasive placenta (AIP). Ultrasound Obstet Gynecol 2016;47(3):271–275.
42. Shainker SA, Coleman B, Timor-Tritsch IE, et al. Special report of the Society for Maternal-Fetal Medicine Placenta Accreta Spectrum Ultrasound Marker Task Force: consensus on definition of markers and approach to the ultrasound examination in pregnancies at risk for placenta accreta spectrum. Am J Obstet Gynecol 2021;224(1):B2–B14. [Published correction appears in Am J Obstet Gynecol 2021;225(1):91.]
43. Alfirevic Z, Tang AW, Collins SL, Robson SC, Palacios-Jaraquemada J; Ad-hoc International AIP Expert Group. Pro forma for ultrasound reporting in suspected abnormally invasive placenta (AIP): an international consensus. Ultrasound Obstet Gynecol 2016;47(3):276–278.
44. D'Antonio F, Iacovella C, Bhide A. Prenatal identification of invasive placentation using ultrasound: systematic review and meta-analysis. Ultrasound Obstet Gynecol 2013;42(5):509–517.
45. Matthews KC, Fields JC, Chasen ST. Suspected Placenta Accreta: Using Imaging to Stratify Risk of Morbidity. Am J Perinatol 2021;38(12):1308–1312.
46. Shih JC, Kang J, Tsai SJ, Lee JK, Liu KL, Huang KY. The "rail sign": an ultrasound finding in placenta accreta spectrum indicating deep villous invasion and adverse outcomes. Am J Obstet Gynecol 2021;225(3):292.e1–292.e17.
47. Palacios-Jaraquemada JM, Bruno CH, Martín E. MRI in the diagnosis and surgical management of abnormal placentation. Acta Obstet Gynecol Scand 2013;92(4):392–397.
48. Familiari A, Liberati M, Lim P, et al. Diagnostic accuracy of magnetic resonance imaging in detecting the severity of abnormal invasive placenta: a systematic review and meta-analysis. Acta Obstet Gynecol Scand 2018;97(5):507–520.
49. Tinari S, Buca D, Cali G, et al. Risk factors, histopathology and diagnostic accuracy in posterior placenta accreta spectrum disorders: systematic review and meta-analysis. Ultrasound Obstet Gynecol 2021;57(6):903–909.
50. Horowitz JM, Berggruen S, McCarthy RJ, et al. When Timing Is Everything: Are Placental MRI Examinations Performed before 24 Weeks' Gestational Age Reliable? AJR Am J Roentgenol 2015;205(3):685–692.
51. Alamo L, Anaye A, Rey J, et al. Detection of suspected placental invasion by MRI: do the results depend on observers' experience? Eur J Radiol 2013;82(2):e51–e57.
52. Ghezzi CLA, Silva CK, Casagrande AS, Westphalen SS, Salazar CC, Vettorazzi J. Diagnostic performance of radiologists with different levels of experience in the interpretation of MRI of the placenta accreta spectrum disorder. Br J Radiol 2021;94(1128):20210827.
53. Zawaideh JP, Freeman S, Smith J, et al. Placental MRI: identification of radiological features to predict placental attachment disease regardless of reader expertise. Eur J Radiol 2022;149:110203.
54. Cal M, Ayres-de-Campos D, Jauniaux E. International survey of practices used in the diagnosis and management of placenta accreta spectrum disorders. Int J Gynaecol Obstet 2018;140(3):307–311.
55. Sannananja B, Ellermeier A, Hippe DS, et al. Utility of diffusion-weighted MR imaging in the diagnosis of placenta accreta spectrum abnormality. Abdom Radiol (NY) 2018;43(11):3147–3156.
56. Ray JG, Vermeulen MJ, Bharatha A, Montanera WJ, Park AL. Association between MRI Exposure during Pregnancy and Fetal and Childhood Outcomes. JAMA 2016;316(9):952–961.
57. ACR Committee on MR Safety. ACR Manual on MR Safety (version 1.0). Reston, Va: American College of Radiology, 2020.
58. Chartier AL, Bouvier MJ, McPherson DR, Stepenosky JE, Taysom DA, Marks RM. The Safety of Maternal and Fetal MRI at 3 T. AJR Am J Roentgenol 2019;213(5):1170–1173.
59. Jaimes C, Delgado J, Cunnane MB, et al. Does 3-T fetal MRI induce adverse acoustic effects in the neonate? A preliminary study comparing postnatal auditory test performance of fetuses scanned at 1.5 and 3 T. Pediatr Radiol 2019;49(1):37–45.
60. Palacios Jaraquemada JM, Bruno CH. Magnetic resonance imaging in 300 cases of placenta accreta: surgical correlation of new findings. Acta Obstet Gynecol Scand 2005;84(8):716–724.

61. Thiravit S, Ma K, Goldman I, et al. Role of Ultrasound and MRI in Diagnosis of Severe Placenta Accreta Spectrum Disorder: an Intraindividual Assessment with Emphasis on Placental Bulge. AJR Am J Roentgenol 2021;217(6):1377–1388.
62. Jha P, Rabban J, Chen LM, et al. Placenta accreta spectrum: value of placental bulge as a sign of myometrial invasion on MR imaging. Abdom Radiol (NY) 2019;44(7):2572–2581.
63. Morlando M, Collins S. Placenta Accreta Spectrum Disorders: Challenges, Risks, and Management Strategies. Int J Womens Health 2020;12:1033–1045.
64. Bour L, Placé V, Bendavid S, et al. Suspected invasive placenta: evaluation with magnetic resonance imaging. Eur Radiol 2014;24(12):3150–3160.
65. Ueno Y, Kitajima K, Kawakami F, et al. Novel MRI finding for diagnosis of invasive placenta praevia: evaluation of findings for 65 patients using clinical and histopathological correlations. Eur Radiol 2014;24(4):881–888.
66. Bourgioti C, Konstantinidou AE, Zafeiropoulou K, et al. Intraplacental Fetal Vessel Diameter May Help Predict for Placental Invasiveness in Pregnant Women at High Risk for Placenta Accreta Spectrum Disorders. Radiology 2021;298(2):403–412.
67. Konstantinidou AE, Bourgioti C, Fotopoulos S, et al. Stripped fetal vessel sign: a novel pathological feature of abnormal fetal vasculature in placenta accreta spectrum disorders with MRI correlates. Placenta 2019;85:74–77.
68. Chen X, Shan R, Zhao L, et al. Invasive placenta previa: placental bulge with distorted uterine outline and uterine serosal hypervascularity at 1.5T MRI: useful features for differentiating placenta percreta from placenta accreta. Eur Radiol 2018;28(2):708–717.
69. Morita S, Ueno E, Fujimura M, Muraoka M, Takagi K, Fujibayashi M. Feasibility of diffusion-weighted MRI for defining placental invasion. J Magn Reson Imaging 2009;30(3):666–671.
70. Romeo V, Ricciardi C, Cuocolo R, et al. Machine learning analysis of MRI-derived texture features to predict placenta accreta spectrum in patients with placenta previa. Magn Reson Imaging 2019;64:71–76.
71. Chen E, Mar WA, Horowitz JM, et al. Texture analysis of placental MRI: can it aid in the prenatal diagnosis of placenta accreta spectrum? Abdom Radiol (NY) 2019;44(9):3175–3184.
72. Do QN, Lewis MA, Xi Y, et al. MRI of the Placenta Accreta Spectrum (PAS) Disorder: Radiomics Analysis Correlates with Surgical and Pathological Outcome. J Magn Reson Imaging 2020;51(3):936–946.
73. Ren H, Mori N, Mugikura S, et al. Prediction of placenta accreta spectrum using texture analysis on coronal and sagittal T2-weighted imaging. Abdom Radiol (NY) 2021;46(11):5344–5352.
74. Palacios-Jaraquemada JM, D'Antonio F, Buca D, Fiorillo A, Larraza P. Systematic review on near miss cases of placenta accreta spectrum disorders: correlation with invasion topography, prenatal imaging, and surgical outcome. J Matern Fetal Neonatal Med 2020;33(19):3377–3384.
75. Shamshirsaz AA, Fox KA, Salmanian B, et al. Maternal morbidity in patients with morbidly adherent placenta treated with and without a standardized multidisciplinary approach. Am J Obstet Gynecol 2015;212(2):218.e1–218.e9.
76. Silver RM, Fox KA, Barton JR, et al. Center of excellence for placenta accreta. Am J Obstet Gynecol 2015;212(5):561–568.
77. Zuckerwise LC, Craig AM, Newton JM, Zhao S, Bennett KA, Crispens MA. Outcomes following a clinical algorithm allowing for delayed hysterectomy in the management of severe placenta accreta spectrum. Am J Obstet Gynecol 2020;222(2):179.e1–179.e9.
78. Gatta LA, Lee PS, Gilner JB, et al. Placental uterine artery embolization followed by delayed hysterectomy for placenta percreta: a case series. Gynecol Oncol Rep 2021;37:100833.
79. Collins SL, Alemdar B, van Beekhuizen HJ, et al. Evidence-based guidelines for the management of abnormally invasive placenta: recommendations from the International Society for Abnormally Invasive Placenta. Am J Obstet Gynecol 2019;220(6):511–526.
80. Matsuzaki S, Yoshino K, Endo M, Kakigano A, Takiuchi T, Kimura T. Conservative management of placenta percreta. Int J Gynaecol Obstet 2018;140(3):299–306.
81. Sentilhes L, Seco A, Azria E, et al. Conservative management or cesarean hysterectomy for placenta accreta spectrum: the PACCRETA prospective study. Am J Obstet Gynecol 2022;226(6):839.e1–839.e24.
82. Youssefzadeh AC, Matsuzaki S, Mandelbaum RS, et al. Trends, characteristics, and outcomes of conservative management for placenta percreta. Arch Gynecol Obstet 2022;306(3):913–920.